Overview of Dual-Active-Bridge Isolated Bidirectional DC–DC Converter for High-Frequency-Link Power-Conversion System

Biao Zhao, *Student Member, IEEE*, Qiang Song, *Member, IEEE*, Wenhua Liu, *Member, IEEE*, and Yandong Sun

Abstract—High-frequency-link (HFL) power conversion systems (PCSs) are attracting more and more attentions in academia and industry for high power density, reduced weight, and low noise without compromising efficiency, cost, and reliability. In HFL PCSs, dual-active-bridge (DAB) isolated bidirectional dc–dc converter (IBDC) serves as the core circuit. This paper gives an overview of DAB-IBDC for HFL PCSs. First, the research necessity and development history are introduced. Second, the research subjects about basic characterization, control strategy, soft-switching solution and variant, as well as hardware design and optimization are reviewed and analyzed. On this basis, several typical application schemes of DAB-IBDC for HPL PCSs are presented in a worldwide scope. Finally, design recommendations and future trends are presented. As the core circuit of HFL PCSs, DAB-IBDC has wide prospects. The large-scale practical application of DAB-IBDC for HFL PCSs is expected with the recent advances in solid-state semiconductors, magnetic and capacitive materials, and microelectronic technologies.

Index Terms—Bidirectional converters, dc–dc conversion, dual active bridge, efficiency, high-frequency link, isolated converters, nanocrystalline magnetic material, power conversion, power density, wide-band-gap semiconductor.

I. Introduction

FOR now, power conversion systems (PCSs) mainly employ line-frequency (LF) transformers to achieve galvanic isolation and voltage matching [1]–[5]. Rapid development of distributed generation and energy storage has led to the increasing popularity of PCSs as an ever-lasting key interface [6]–[10]. However, bulky, heavy, lossy, and noisy LF transformers hinder the efficiency and power density of PCSs.

In recent years, the use of high-frequency (HF) transformers in place of traditional LF transformers is considered to be the developing trend of next-generation power conversion. Fig. 1 shows a comparative photo of 50-Hz LF and 20-kHz HF transformers. The advantages of HF transformers are low
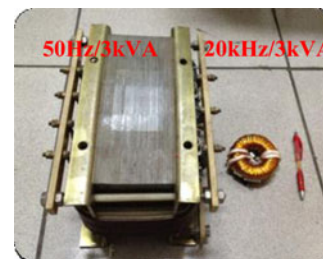
Fig. 1. Comparative photo of 50-Hz LF and 20-kHz HF transformers.

volume, light weight, and low cost. And high-frequency-link (HFL) PCSs based on HF transformers can also avoid voltage and current waveform distortion caused by the core saturation of LF transformers. In addition, when the switching frequency is above 20 kHz, PCS noise can be greatly reduced. Especially, in the background of rapid expand of PCS, HFL-PCSs have wide application prospects.

In the research of HFL-PCSs, isolated bidirectional dc–dc converters (IBDCs) usually serve as the key circuit. Generally, all of IBDCs can be evolved from traditional isolated unidirectional dc–dc converters (IUDCs), such as: flyback IUDC can compose dual-flyback IBDC, half-bridge or push–pull IUDC can compose dual-half-bridge or dual-push–pull IBDC, and full-bridge IUDC can compose dual-active-bridge IBDC. In fact, besides the IBDCs composed of IUDCs with the same type, the IUDCs with different types also can compose IBDCs, such as half-bridge IUDC and push–pull IUDC can compose a half-bridge-push-pull IBDC because the half-bridge and push-pull structures can withstand high- and low-source voltages, respectively, so this type of IBDC can be used in the application with a wide voltage range and a bidirectional power flow. Similar to the classification of traditional dc–dc converters in power electronics, this paper presents a classification of IBDC topology based on the number of switches, as shown in Table I. The simplest IBDC topology is a dual-switch structure, such as: dual-flyback IBDC, dual-Cuk IBDC, and Zeta-Sepic IBDC [11]–[14]. The typical model of three-switch topology is forward-flyback IBDC [15]. Four-switch topologies mainly contain dual-push-pull IBDC, push-pull-forward IBDC, push-pull-flyback, and dual-half- bridge IBDC [16]–[24]. The typical model of five-switch topology is full-bridge-forward IBDC [25]. The typical model of six-switch topology is half-full-bridge IBDC [26]. Eight-switch topology is mainly dual-active-bridge IBDC (DAB-IBDC) [27]–[29].

TABLE I
CLASSIFICATION OF IBDC TOPOLOGY

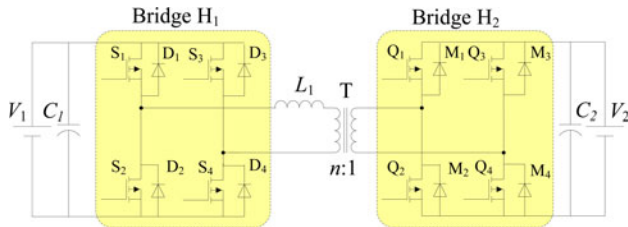| Classification I	Number of switches					
	Dual-switch	Three-switch	Four-switch	Five-switch	Six-switch	Eight-switch
Typical models	dual-flyback, dual-Cuk, Zeta-Sepic	forward-flyback	dual-push-pull, push-pull-forward, push-pull-flyback, dual-half-bridge	full-bridge-forward	half-full-bridge	dual-active-bridge

Fig. 2.   Topology of DAB-IBDC.

Overall, IBDC topologies for HFL-PCSs are numerous and diverse. But, in general, when the rated voltage and current of switches are the same, the transmission power of IBDC is proportional to the number of switches, such as the power capacity of four-switch IBDC is double that of dual-switch IBDC but half that of eight-switch IBDC, so the DAB-IBDC has the biggest power capacity. And from the view of filter, the output pulsation frequency for forward converter is switching frequency but for the push–pull, half-bridge and full-bridge converters is double switching frequency, so with the same output voltage, the filter for DAB-IBDC is also small. Moreover, the DAB-IBDCs have the advantages of ease of realizing soft-switching, bidirectional power transfer capability, and modular and symmetric structure, etc., so they are attracting more and more attentions in recent years. In 2007, [30] and [31] present that DAB-IBDC will be served as the core circuit for next-generation HFL PCSs. The viewpoints have also been recognized by most researchers. Fig. 2 shows the topology of DAB-IBDC, which composes of two full-bridge converters, two dc capacitors, an auxiliary inductor, and an HF transformer. The HF transformer provides the required galvanic isolation and voltage matching between two voltage levels. The auxiliary inductor serves as the instantaneous energy storage device.

In fact, DAB-IBDCs were proposed in the early 1990s [32]–[34]. However, because of the performance limitations of power devices, the power losses of DAB-IBDCs were high and the efficiency was unacceptable. Hence, DAB-IBDC did not reach a new stage of development, and related research literature were few [35]–[37]. In recent years, the advances in new power devices and magnetic materials (especially the development of silicon carbide (SiC)- and gallium-nitride (GaN)-based power devices and iron-based nanocrystalline soft magnetic) have made DAB-IBDC feasible for eliminating bulky and heavy LF transformers from PCSs [38], [39]. Thus, DAB-IBDC has regained the attention of numerous researchers.

Thus far, studies on DAB-IBDC mainly focus on the following aspects: basic characterization, control strategy, soft-switching solution and variant, and hardware design and optimization. In view of this research situation, this paper will give
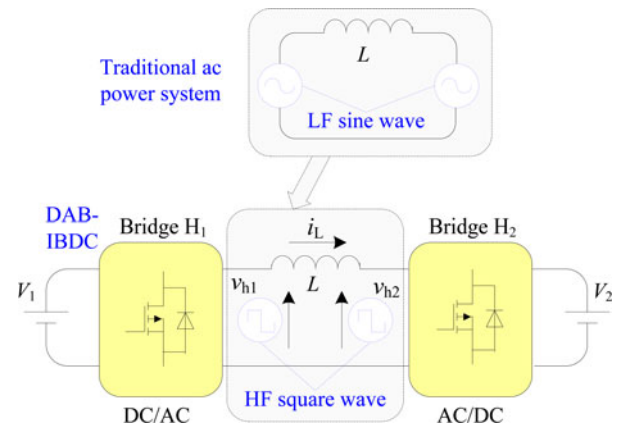

Fig. 3.   Basic principles of traditional ac power system and DAB-IBDC.

an overview of DAB-IBDC. On this basis, the typical applications of DAB-IBDC for HFL PCSs and future trends will be discussed.

This paper is organized as follows. Section II introduces the basic characterization research of DAB-IBDC. Section III analyzes a representative part of control strategies, which are the most widely studied methods for DAB-IBDC. Section IV discusses the soft-switching solution and variant. Section V discusses the hardware design and optimization. Section VI analyzes several typical application schemes of DAB-IBDC for HPL PCSs. Finally, Section VII discusses design recommendations and future trends.

II. BASIC CHARACTERIZATION

A. Basic Principle

The comprehensive analyses of the operation, design, and control of DAB-IBDC in steady state were introduced in [40] and [41], and a boundary control scheme for DAB-IBDC using the natural switching surface is present in [42]. Literature [43] discussed the short-time-scale transient processes with phase-shift control and proposed a set of strategies to increase system robustness.

Fig. 3 shows that similar to the control of the power transmission in traditional ac power systems, the direction and magnitude of the inductor current i_L can be changed by adjusting the phase shift between ac output square wave voltages v_{h1} and v_{h2} of bridges H_1 and H_2, which can control the direction of power flow and magnitude of DAB-IBDC. The difference is that the voltages in both sides of the inductor in traditional ac power system are line-frequency sinusoidal waves and in DAB-IBDC are high-frequency square waves. The transmission power models
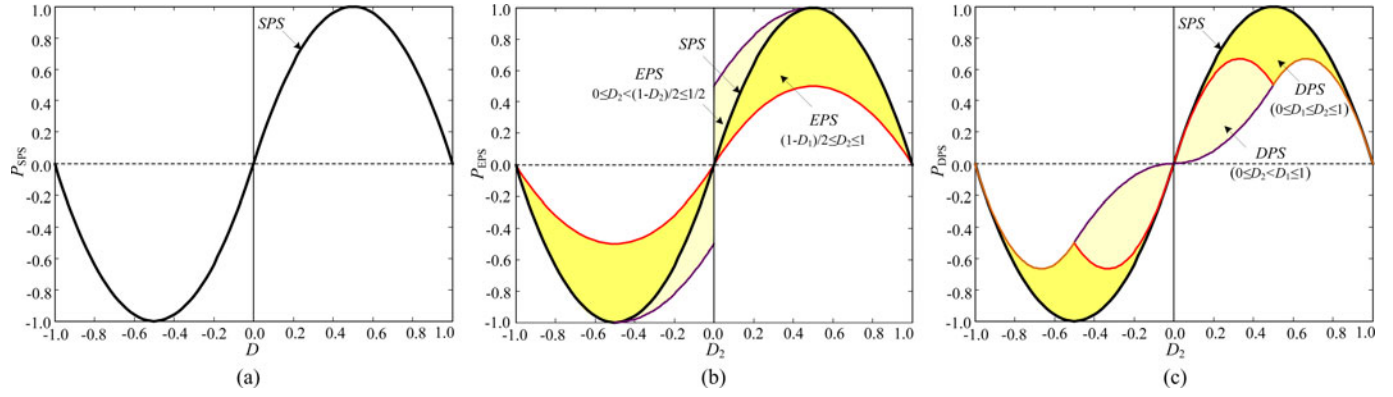
Fig. 4. Transmission power characterization of DAB-IBDC. (a) SPS control. (b) EPS control. (c) DPS control.

of the traditional ac power system and of DAB-IBDC can be derived as

$$\begin{cases} P_{\text{sine}} = \dfrac{V_{\text{rms1}} V_{\text{rms2}}}{2\pi f_s L} \sin \varphi \\ P_{\text{square}} = \dfrac{n V_1 V_2}{2\pi^2 f_s L} \varphi(\pi - \varphi) \end{cases} \quad (1)$$

where V_{rms1} and V_{rms2} are the root mean square (RMS) of sinusoidal waves, and φ is the phase shift between ac voltages.

In fact, because of the high-frequency power transmission, the power density and modularity improve significantly. Hence, DAB-IBDC is considered as the core circuit of the HFL-PCSs attracting a lot attention. Aside from these basic characteristics, the studies on DAB-IBDC also focus on transmission power characterization, deadband effect, and dynamic model.

B. Transmission Power Characterization

The basic transmission power characterization of DAB-IBDC with a single-phase-shift (SPS) control is shown in Fig. 4(a), where $D = \varphi/\pi$ is the phase-shift ratio [40]. From Fig. 4(a), several conclusions can be drawn: the transmission power relation curve is symmetric around the median axis $D = 0.5$, the zero and maximum points of the transmission power are achieved at $D = 0$ and $D = 0.5$, respectively, and the transmission power increases with the increase of D when $D \leq 0.5$ and the decrease of D when $D > 0.5$. These conclusions are usually used to provide reference for the power prediction and design.

On this basis, the transmission power characterizations with extended-phase-shift (EPS) and dual-phase-shift (DPS) controls were discussed in [44]–[46]. In [26], the conclusion is also derived that the DPS control cannot increase the maximum transmission power capacity, which corrects the conclusion obtained in [46] that the maximum output power is 4/3 times that of the SPS control. The regulating range of transmission power changes from a single curve in Fig. 4(a) to the two-dimensional area in Fig. 4(b) and (c) due to the addition of an inner phase-shift ratio D_1. The EPS and DPS controls, with the same outer phase-shift ratio $(D_2 = D)$, offer a wide power transmission range, which enhances regulating flexibility. In addition, when $D_2 = D < 0.5$, compared with SPS and DPS controls, the EPS control can increase the transmission power capacity by adjusting D_1.

The timing diagrams of SPS, EPS, and DPS control are shown in Fig. 5, which will be further discussed in Section IV.

C. Deadband Effect

In the last section, the characterization does not consider the effects of deadband. But in practice, the deadband must be set to prevent shorting the two switches in the same leg, an effect that will cause the change of switching characterization.

Literatures [47], [48] presented a comprehensive theoretical analysis and experimental verification of the deadband effect in DAB-IBDC. Moreover, literatures [49], [50] also discussed the deadband control methods to expand soft-switching range and increase the efficiency of IBDC. The voltage polarity reversal and voltage sag phenomena caused by deadband effect were shown in Fig. 6. On this basis, the transmission power characterization can be corrected, as shown in Fig. 7, where M is the deadband ratio in a half-switching period. A phase-drift phenomenon appears in the transmission power characterization because of the addition of deadband; that is, the transmission power remains constant with the increase of D in a certain range and begins to change approximately when phase-shift time is greater than dead time.

D. Dynamic Model

The design of the controller requires a small-signal average model. The dynamic model analyses of DAB-IBDC were studied in [41], [51]–[56]. Fig. 8 shows the equivalent circuits of average and small-signal models in [41]. Literatures [51]–[53] discussed the simplified reduced-order model, which neglects the transformer current dynamic. Considering the leakage inductance current and the resonant transition intervals, the full-order small-signal modeling and dynamic analysis of zero-voltage-switching (ZVS) phase-shift DAB-IBDC was studied and a general modeling method to develop the discrete time average model was proposed in [54]. And an accurate small-signal model including electromagnetic-interference (EMI) filter for the digital control of an automotive DAB-IBDC was derived in [55]. Literature [56] used the dc terms and first-order terms of transformer current and capacitor voltage as state variables to study the full-order continuous-time average modeling and dynamic analysis, which results in a third-order model if a
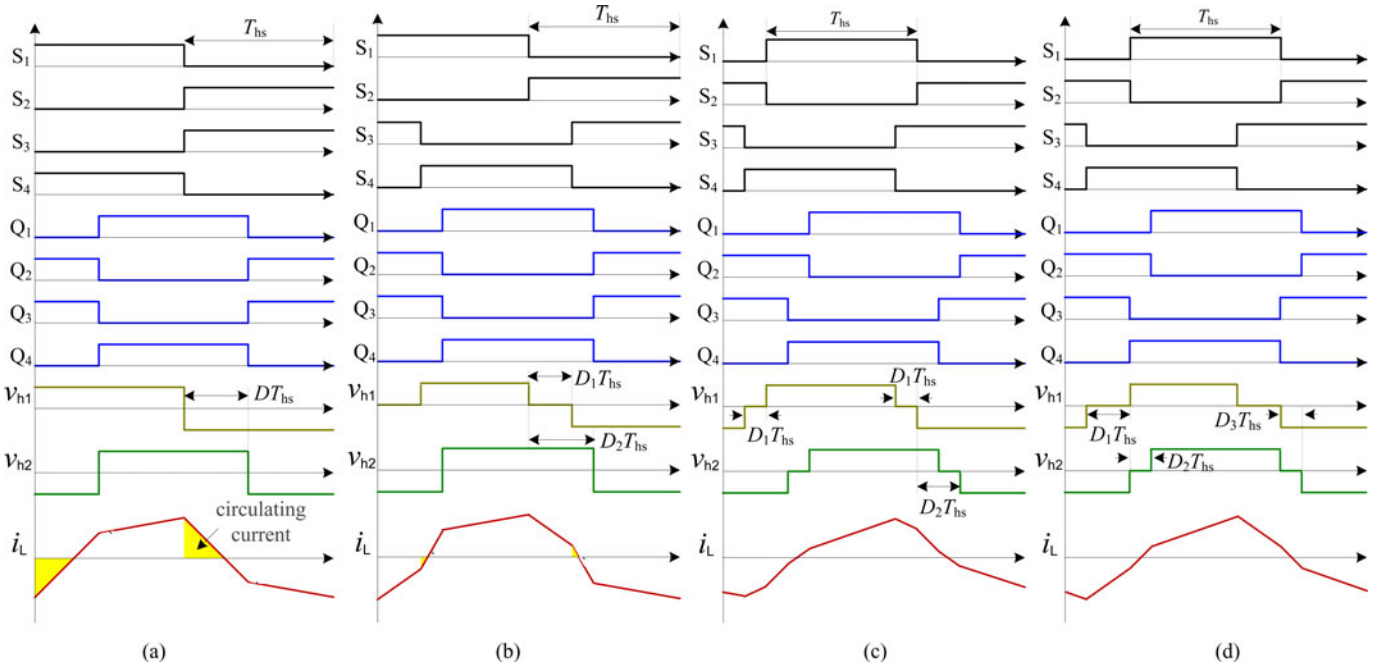
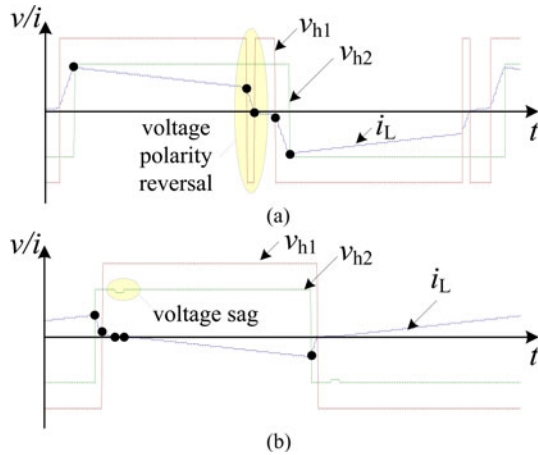Fig. 5.   (a) SPS control. (b) EPS control. (c) DPS control. (d) TPS control.

Fig. 6.   (a) Voltage polarity reversal phenomenon of DAB-IBDC. (b) Voltage sag phenomenon of DAB-IBDC.

Fig. 7.   Improvement of transmission power characterization with deadband effect.

capacitor equivalent series resistance (ESR) is not considered, and a sixth-order model if ESR is considered.

Usually, the full-order discrete-time model can obtain higher accuracy at low frequencies than a reduced-order model. However, a continuous-time model is usually preferred because it provides more physical insight and facilitates control design [56].

III. CONTROL STRATEGY

Control strategy is one of the important research directions for DAB-IBDC. In this section, we introduce and analyze a representative part of the control methods, which are the most widely studied methods for DAB-IBDC. In fact, for improved topologies and variant, the control methods may be different, but all of these methods can be derived from the following methods.
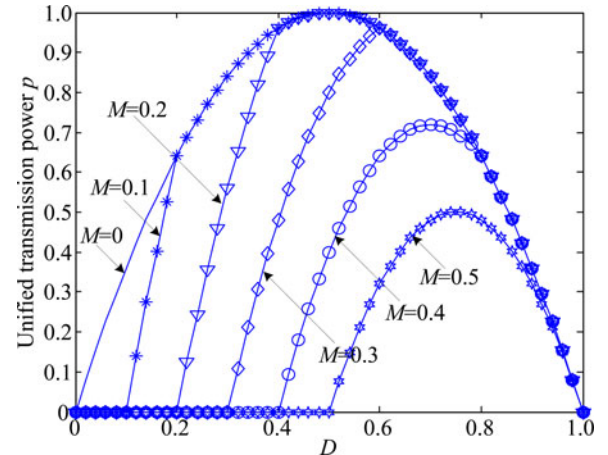
A. SPS Control

The most widely used control method for DAB-IBDC is SPS control [30]–[34], [40], [43], [57] which is shown in Fig. 5(a). In Fig. 5, S_1–S_4 and Q_1–Q_4 are square-wave gate signals with 50% duty ratio for the corresponding switches in Fig. 2. v_{h1} and v_{h2} are the equivalent ac output voltages of full-bridges H_1 and H_2, respectively, and i_L is the current of inductor L.

In SPS control, the cross-connected switch pairs in both full bridges are switched in turn to generate phase-shifted square waves with 50% duty ratio to the transformer's primary and secondary sides. Only a phase-shift ratio (or angle) D can be controlled. Through adjusting the phase-shift ratio between v_{h1} and v_{h2}, the voltage across the transformer's leakage inductor will change. Then, the power flow direction and magnitude can simply be controlled.
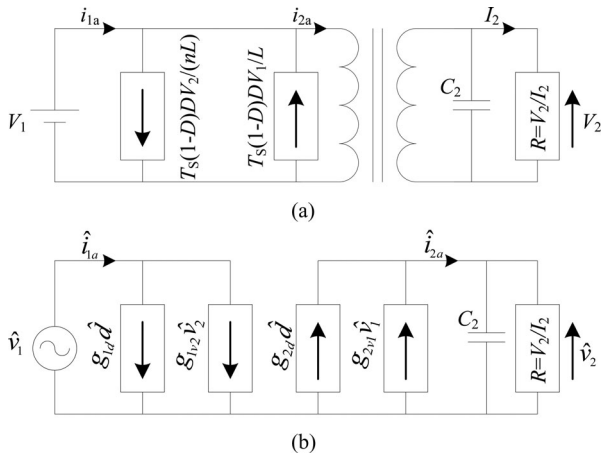
Fig. 8. Equivalent circuits of dynamic models in [41]. (a) Average model. (b) small-signal model.

SPS control is attracting more and more attention due to its advantages, such as small inertia, high dynamic, and ease of realizing soft-switching control, and so on. However, in this method, the control of the power flow depends on the transformer's leakage inductor that result in great circulating power when the voltage amplitude of two sides of the transformer is not matched, then both the RMS and peak current increase. Moreover, the converter cannot operate under ZVS in the whole power range in this situation. Therefore, the power loss becomes much higher, and its efficiency is greatly reduced.

B. EPS Control

EPS control is a typically improved method of SPS control, as shown in Fig. 5(b). In EPS control, the cross-connected switch pairs in one full bridge are switched in turn, while switch pairs in another bridge are switched with an inner phase-shift ratio. Then, the output ac voltage of one bridge becomes a three-level wave while the other one is two-level 50% square wave. During the time intervals of the zero voltage of the three-level wave, the backflow power is 0, so the circulating power decreases for a given transmission power.

The operation principle and the performance of transmission power, current stress, power loss, and soft switching for the EPS control are discussed in [44], [58]–[61]. Compared with SPS control, EPS control not only improves efficiency and expands the ZVS operation range, but also reduces the current stress and enhances the regulating flexibility.

In fact, compared to the single phase-shift ratio D in the SPS control, there is not only the outer phase-shift ratio D_1 but also the inner phase-shift ratio D_2 in the EPS control. Outer phase-shift ratio is used to control the power flow direction and magnitude, whereas the inner phase-shift ratio is used to decrease circulating power and expand ZVS range. But for the EPS control, when the voltage conversion states are changed between the boost and buck states and the power flow directions are changed between the forward and reverse power flow, the operating states of the two bridges are needed to be exchanged to achieve the decreased circulating power.

C. DPS Control

Similar to the EPS control, the DPS control was proposed in [27], as shown in Fig. 5(c). Different with the EPS control, in DPS control, the cross-connected switch pairs in both full bridges are switched with an inner phase-shift ratio, and the inner phase-shift ratios are the same. Then, the output ac voltages of both bridges are three-level waves.

The operation principle, transmission power, current stress, power loss, and soft switching, and optimization design methods for the DPS control were discussed in [45], [46], [53], [62]–[64]. Compared with the SPS control, DPS control can decrease current stress and steady-state current, improve efficiency, expand the ZVS operation range, and minimize the output capacitance. Under certain operation conditions, deadband compensation can also be implemented easily in the DPS control without a current sensor.

Compared with the EPS control, the operating states of the two bridges will be the same when the voltage conversion states or power flow directions are changed. Hence, DPS control is easier to implement, and its dynamic performance may be more excellent.

D. Triple-Phase-Shift (TPS) Control

The TPS control was proposed in [55], [65]–[70] as shown in Fig. 5(d). Similar to the DPS control, the cross-connected switch pairs in both full bridges are switched with an inner phase-shift ratio. However, the inner phase-shift ratios may be unequal. TPS control can also control three degrees of freedom.

Hence, research on TPS control mainly focuses on the optimization operation field. Literature [55] investigated small-signal model for the digital control of DAB-IBDC with TPS control. An optimal modulation scheme that enables minimum conduction and copper losses was presented for DAB-IBDC with TPS control in [65]. Based on this, an efficiency-optimized modulation scheme and corresponding design method were developed for an existing DAB-IBDC prototype in [66]. A hybrid modulation scheme and a feedback-linearized control were designed to extend the power range for ultracapacitor application in [67]. An optimal modulation strategy for reverse-mode operation of TPS control was analyzed in [68]. A stability analysis method to make the stability determination of DAB-IBDC with TPS control more systematic and precise was discussed in [69]. In addition, a comprehensive analysis and experimental verification with pulse width modulation (PWM) control were proposed in [70], and a composite scheme of TPS control was explored that extends the soft-switching range down to zero-load condition, reduces RMS and peak currents, and results in significant size reduction of the transformer.

In fact, the TPS control was proposed after SPS, EPS, and DPS control; it is a unified form of phase-shift control. SPS, EPS, and DPS control can also be regarded as special cases of TPS control. From the view of implementation, SPS control requires only one control degree; the EPS and DPS control require two control degrees, and three control degrees are needed for TPS control. Hence, TPS control is the most difficult to implement, and there is also not a unified implement standard at present.
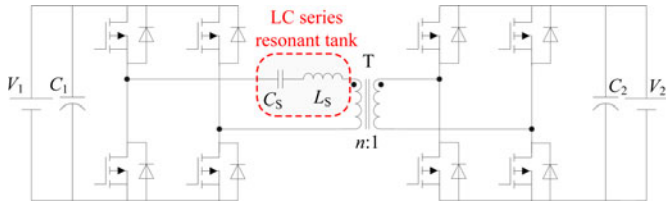
Fig. 9.   *LC*-type resonant DAB-IBDC in [74].

For EPS control, the operating states of the two bridges should be changed when the voltage conversion states or power flow directions are changed. And for the SPS control, the efficiency, ZVS range, etc., have flaws. So DPS control may be relative optimal method for the large-scale practical application from the implementation difficulty and performance.

IV. SOFT-SWITCHING SOLUTION AND VARIANT

A. Soft-Switching Solution

DAB-IBDCs have the advantages of ease of realizing soft-switching, bidirectional power transfer capability, and modular and symmetric structure, etc., so they are attracting more and more attentions in recent years. However, the circulating current becomes much higher and the efficiency decreases rapidly when the voltage amplitude of the two sides of the transformer do not match [44], [46], [71]. Moreover, the soft-switching range decreases under light load [72], [73]. To address these problems, the soft-switching solution is a research direction to improve the performance, and so far, the general research ideas focus on the improvement of HFL resonant tank to expand the soft-switching range of DAB-IBDC. This section gives three typical solutions in literatures to discuss the soft-switching solution of DAB-IBDC.

Fig. 9 shows a LC-type resonant topology based on DAB-IBDC [74]. Compared to traditional DAB-IBDC, the converter can be operated at higher frequency and efficiency due to its advantages of operation, but additional resonant components also bring extra size and cost. In [74], the control method for the converter is phase-shift control with fixed frequency (all the switches in both full bridges are driven with 50% duty cycle), and two ac equivalent (with fundamental component) circuit analysis approaches are used for the purpose of design. *LC*-type resonant DAB-IBDC shares similarities with the traditional series resonant unidirectional full-bridge dc–dc converter and still has some unique features due to the secondary-side bridge, such as the capability of bidirectional power flow. From soft-switching performance, ZVS for primary-side switches and ZCS for secondary-side switches could be achieved.

Fig. 10 shows a CLLC-type asymmetric resonant topology based on DAB-IBDC [75]. Both the power flow directions are modulated under variable frequency modulation above resonance, and the inverter switches are driven with 50% duty cycle and the rectifier switches are driven by the additional resonant signals. Similar to the *LC*-type converter above, ZVS for inverter switches and ZCS for rectifier switches could be achieved for a wide variation of voltage gain.
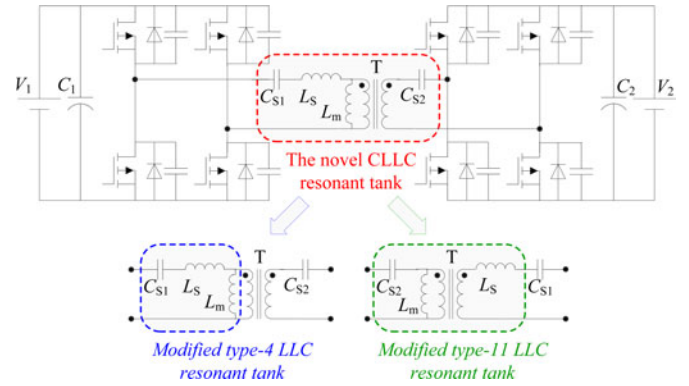

Fig. 10.   CLLC-type asymmetric resonant DAB-IBDC [75].
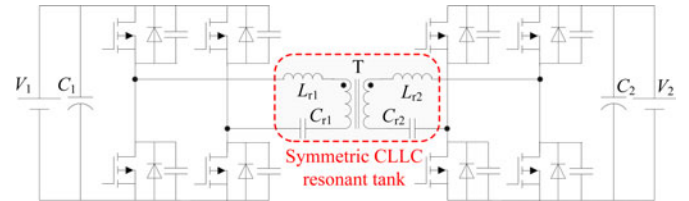

Fig. 11.   CLLC-type symmetric resonant DAB-IBDC in [76].

On this basis, several literatures also analyzed the symmetric resonant DAB-IBDC. A DAB-IBDC using a new symmetric CLLC-type resonant network is shown in Fig. 11 [76]. The power flow direction is determined by the position of the switches' operating stages. The power switches are driven with 50% duty cycle and generate ac power to the transformer in the inverting stage. In the rectifying stage, all the switches are turned OFF and the transferred power is rectified by antiparallel diodes of the switches. Similar to the CLLC-type asymmetric converter above, the transmission power and the output voltage are also modulated under variable frequency modulation. This converter can operate under high-power conversion efficiency because the symmetric CLLC resonant network has ZVS capability for inverter switches and soft commutation capability for rectifier switches [77]. And the power conversion operation and its efficiency are exactly the same as other power flow directions.

Table II gives comparison of different soft-switching solutions. From Table II, with different topologies, the control strategies are different, which also cause the different soft-switching performance. Compared to the traditional and *LC*-type resonant DAB-IBDCs, the CLLC-type resonant converters employ frequency modulation that increases the control difficulty and the CLLC network requires more resonant components that bring higher size and cost. In addition, from the transition speed of bidirectional power flow, the direction of CLLC-type converters is determined by the position of the switches' operating stage, but the traditional and LC-type DAB-IBDCs are easily controlled by phase-shift angle through phase-shift control, so the bidirectional transition speed of phase-shift control is faster. However, from soft-switching range, the CLLC-type resonant converters has wider soft-switching range than traditional and *LC*-type DAB-IBDCs, so they are more suitable for applications with wide voltage and power range. In addition, because

TABLE II
COMPARISON OF DIFFERENT SOFT-SWITHCING SOLUTIONS

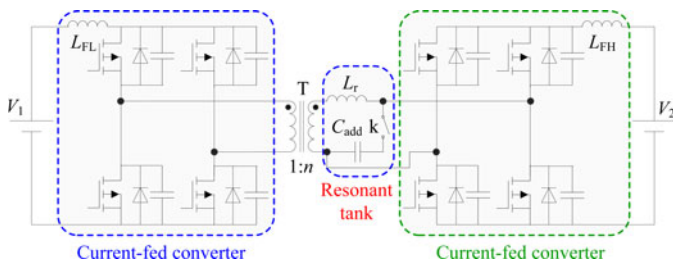| Converter	Resonant network structure	Power control	Drive	Soft-switching characterization	Soft-switching range	Additional component	Bidirectional transition speed
Traditional-type	No	Phase-shift modulation	50% duty cycle for all switches	ZVS for few switches	Narrow	No	Fast
LC-type resonant	Series resonant tank	Phase-shift modulation	50% duty cycle for all switches	ZVS for primary switches, ZCS for secondary switches	Narrow	A capacitor	Fast
CLLC-type asymmetric resonant	Series-parallel resonant tank	Frequency modulation	50% duty cycle for inverter switches, additional resonant signals for rectifier switches	ZVS for inverter switches, ZCS for rectifier switches	Wide	Two capacitors and a inductor	Slow
CLLC-type symmetric resonant	Series resonant tank	Frequency modulation	50% duty cycle for inverter switches, turn off for rectifier switches	ZVS for inverter switches, soft commutation for rectifier switches	Wide	Two capacitors and a inductor	Slow

Fig. 12.   Current-current-fed resonant DAB-IBDC in [78].

Fig. 13.   Three-phase DAB-IBDC in [32], [86]–[90].

TABLE III
COMPARISON OF SINGLE-PHASE AND THREE-PHASE DAB-IBDC [32]

Converter	Number of switches	Peak current/A	Peak voltage/V	Transformer kVA	Cap. Rms current/A
Single-phase	8	297.57	2000	56.28	12.92
Three-phase	12	293.46	2000	55.7	4.84

the turn numbers of the transformer and the structure of the resonant networks are asymmetric, the CLLC-type asymmetric resonant converter shows different operations between forward and backward power flow directions compared to symmetric resonant converter.

Besides the representative solutions with voltage-voltage-fed*converters, some studies also discussed the soft-switching solution based on current-fed DAB-IBDC. Here gives a typical topology as an example, as show in Fig. 12. A current-current-fed resonant DAB-IBDC is proposed in [78], which consists of two class-E resonant converters. An additional capacitor C_{add} is introduced by closing the key k during the power transfer from the LV side to the high-voltage (HV) side. The LV converter transistors are controlled and the converter operates as a class-E boost converter [79], whereas the HV converter transistors are not controlled and the converter operates as a class-E rectifier composed of transistor body diodes. The bidirectional power flow is controlled by control pulse frequency changes. The boost or buck operation depends on the mutual relation between the control pulses of the switch pairs, which are located diagonally in the bridge. The main advantages of the converter are high-operation frequency and zero value of the switching losses. However, the converter control is complex, the experimental efficiency in [78] is not satisfactory, and the further studies for the performance of the converter are required.
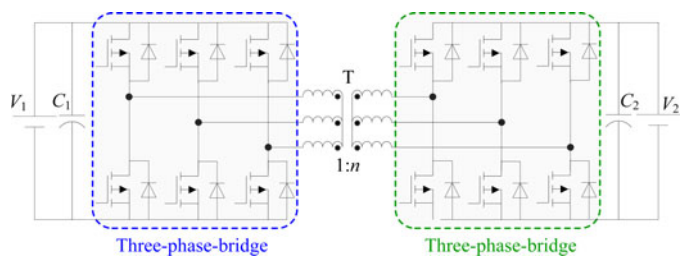
B. Topology Variant

According to different applications, the traditional DAB-IBDC also has many variants [80]–[97]. Here gives two variants as typical examples.

As shown in Fig. 13, a three-phase DAB-IBDC is proposed [32], [86]–[90]. This topology works in the same manner as the single-phase DAB-IBDC, the different is that each full bridge in single-phase converter is operated in a two-level mode but in three-phase converter is operated in a six-step mode with controlled phase shift. Table III gives a comparison of both converters with transmission power 50 kW, input voltage 200 V, output voltage 2000 V, and switching frequency 50 kHz. It can be seen that the three-phase converter has a slightly lower device stresses than single-phase converter. Similar conclusions are seen from the transformer kilovoltampere (kVA) ratings. In addition, the three-phase converter dramatically reduces the capacitor ripple currents because of the higher ripple frequency and makes redundant operation possible by the two additional phase legs. However, the biggest disadvantage for three-phased
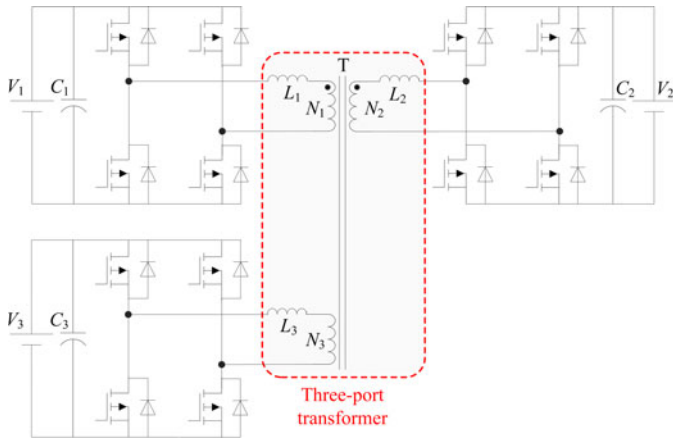
Fig. 14.   Multiports DAB-IBDC in [91]–[97].

Fig. 15.   Optimization design of magnetic components. (a) Auxiliary inductor and transformer. (b) Integration magnetic module.

DAB-IBDC is the practical realization of a three-phase symmetrical transformer with identical leakage inductances in each phase [32]. In addition, it requires more power and magnetic devices that increase the size and cost. So the three-phase DAB-IBDC is recommended for high-power application.

In addition, since a dc–dc converter can connect any two ports, it is natural to think of linking multiports up either by multi-individual dc–dc conversion stages with a common link, where energy from all ports is exchanged. Fig. 14 shows a three-port DAB-IBDC in [91]–[97]. The transformer not only integrates and exchanges the energy from and to all ports, but also provides full isolation among all ports and matches the different port voltage levels. The control method of the multiport DAB-IBDC is the same as the two-port DAB-IBDC. The current stress and circulating conduction loss also become much higher when the voltage amplitudes of the two sides of the transformer do not match. Similarly to the two-port DAB-IBDC research, many variants have been presented, such as half-bridge multiport type, current-fed multiport type, three-phase multiport type, and so on [95]–[97].

V. HARDWARE DESIGN AND OPTIMIZATION

Hardware design is an important research direction of DAB-IBDC; it mainly focuses on the optimization design of parameters, magnetic components (transformer and inductor), power devices, and hardware structure.

A. Main Parameters

A power loss model of LV and high-current DAB-IBDC for automotive applications was analyzed in [98]. Some design suggestions were also presented to achieve high efficiency. On this basis, an efficiency-optimized design method was developed for an existing DAB-IBDC prototype for an automotive application in [66]. The design procedure is given that the optimization of the modulation scheme is the first step toward a complete optimization, and the calculation of the optimal hardware parameters of transformer turn ratio and auxiliary inductance is the second step. Literatures [63], [64] analyzed the general efficiency and current-stress optimization switching strategies of DAB-IBDC
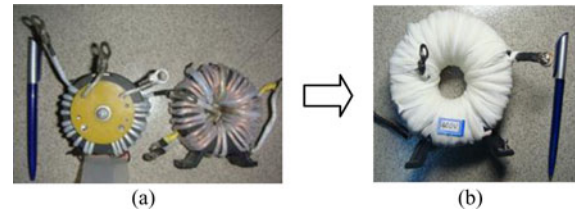
with DPS control; the methods used are particularly effective for operation conditions with big voltage conversion ratio and light load. But the optimization methods based on mathematical models may be limited in accuracy. Literature [99] proposed a parameter- optimization method of DAB-IBDC based on advanced components, in which the optimal parameters focus on the auxiliary inductance and switching frequency. Usually, the main parameters for DAB-IBDC needed to be determined are as follows, input and output voltages, rating power, transformer turn ratio, auxiliary inductance (included transformer leakage inductance), and switching frequency.

B. Magnetic Components

High-frequency transformer is the most key component for DAB-IBDC, which has a direct impact on the performance. Literature [100] analyzed the nature of the problem with experimental determination of approximate lumped parameter modeling and saturation behavior of the transformer, and proposed a simple closed-loop control algorithm with online tuning of the controller parameters to improve transformer utilization. To optimize winding configurations of the transformer, a hybrid method of particle swarm optimization and differential evolution was proposed in [101].

Besides the operation optimization above, the structure optimization of the transformer is also a research direction. In order to improve the operation performance of DAB-IBDC at light load, a transformer with dual leakage inductor and variable frequency was proposed in [102]. The proposed dual leakage transformer has a winding configuration that yields a high leakage inductance at low currents and low leakage inductance at high currents. Similar to [102], an adaptive inductor was proposed as the main energy transfer element in [103]. Output current was used as the bias current of inductor. Thus, the inductance could be automatically optimized over output power to maintain ZVS at light load and to minimize the conduction losses at heavy load.

In [104], auxiliary inductance is obtained by placing the leakage layer, which is made of standard 3F3 ferrite slabs, on top of the secondary winding to increase power density. And literature [105] used the separate winding layout structure with an inserted thin insulation layer between two C core pairs to obtain auxiliary inductance and high insulation voltage. In fact, as shown in Fig. 15, integrating the auxiliary inductor and transformer into a single module is recommended to increases the power density and modularity of IBDC.

Parameter	Nanocrystalline	Ferrite
Saturation magnetic flux density Bs (T)	1.25	0.5
Residual magnetic flux density Br (T)	<0.2	0.2
Iron loss (20KHz/0.2T) (W/Kg)	<3.4	7.5
Iron loss (20KHz/0.5T) (W/Kg)	<35	--
Iron loss (50KHz/0.3T) (W/Kg)	<40	--
Magnetic permeability	>20000	2000
Coercive force Hc (A/m)	<1.6	6
Curie temperature (℃)	570	<200

TABLE V
COMPONENTS COMPARION OF THREE DAB-IBDCS IN [112]

Main components	DAB-IBDC with state of art components	DAB-IBDC with available advanced components	DAB-IBDC with future component
LV switches	MOSFET R_{on}=2.8mΩ t_{on}/t_{off}=135/150ns	DirectFET MOSFET R_{on} =1.7mΩ t_{on}/t_{off} =50/10ns	GaN R_{on} =0.17 mΩ t_{on}/t_{off} =5/1ns
HV switches	IGBT SK80MD055	Discrete Si MOSFET, SiE806DF	GaN, 10X smaller R_{on} 10X smaller t_{on}/t_{off}
Magnetics	3C90	3F3	10X smaller loss density than Nanocrystalline
Input/output cap	Al. Electrolytic	MLCC(X7R)	10X higher energy density

Usually, high-frequency transformer cores in DAB-IBDC are mainly made of ferrite. But the ferrite has the low-saturation magnetic flux density, magnetic permeability, and Curie temperature, which cause the relatively big volume, poor temperature properties, and unstable operation states for the magnetic components. Moreover, high-production difficulty of high-power ferrite drives up the production costs, and leads to high price. Advanced magnetics materials are attracting more and more attention in recent years, and iron-based nanocrystalline soft-magnetic material is one of the most concerns [99]. Table IV shows rough characteristics comparison of iron-based nanocrystalline and ferrite materials. Compared to ferrite, the iron-based nanocrystalline material generally has higher saturation magnetic flux density, magnetic permeability, and Curie temperature and lower iron loss, so it has better development prospects in HFL PCSs. Literature [106] discussed the optimization design method of low-profile nanocrystalline transformer, which focuses on the core dimension optimization and leakage inductance tune to decrease loss.

C. Power Devices

In order to improve the performance of efficiency and power density, many literatures discussed the application of wideband gap (WBG) power devices for DAB-IBDC.

Switch-series-type high-voltage DAB-IBDCs based on Si and SiC JFET devices were compared in [107]. The good material characteristic of SiC-JFET and the resulting high operating frequency led to a compact and low loss system. Literature [108] analyzed the performance of DAB-IBDC based on enhancement-mode GaN-on-silicon) transistors. The analysis showed that GaN devices are capable of outperforming Si devices for the primary bridge, and on the secondary side, GaN devices perform largely on-par with Si devices. High-frequency design considerations of DAB-IBDC based on SiC devices were discussed in [109]. And sample devices are 1200-V/20-A SiC MOSFETs copacked with 10-A JBS diodes manufactured by CREE Inc. Literature [110] analyzed the application performance characteristics and basic design procedure of DAB-IBDC based on SiC-doublediffusion metal-oxide-semiconductor (DMOS) and silicon carbide-Schottky barrier diode samples provided by ROHM Inc., and literature [111] gave an experimental comparison of DAB-IBDC based on all-Si and

all-SiC power devices for HFL PCS. On this basis, the optimization design method of high-efficiency and high-density SiC-based DAB-IBDC was proposed in [99]. The analysis shows that the SiC-based DAB-IBDC has satisfactory performances that are expected to be applied in next-generation HFL PCSs.

In fact, literature [112] surveyed the recent material development of key components in PWM converters and compared the power densities of air-cooled DAB-IBDC with three categories of components, namely state-of-the-art components, available advanced components and future components. The main components used in three DAB-IBDCs are listed in Table V. According to the analysis in [112], the DAB-IBDC with future components can double the power density of the DAB-IBDC with available advanced components. In addition, the loss analysis in [30] clarifies that the efficiency of DAB-IBDC with mature SiC power devices may reach 99% by 2015.

In fact, in WBG semiconductor materials, SiC and GaN have entered the device research stage from that of material. Compared with GaN, SiC has higher thermal conductivity, SiC monocrystalline is easier to produce and the price is lower, so SiC power devices have more advantages in high-temperature and high-power applications, which may be more expected to high-power DAB-IBDC applications [99]. Recent years, developing GaN on Si substrate is becoming a trend, the research show the tremendous potential of GaN hetero structures grown on Si for very high-voltage applications, once that the Si substrate has been removed, and the removal of Si substrate can be integrated with the packaging of the device, which will reduce cost and increase performance [113].

D. Hardware Structure

Hardware structure has an effect on the power density of DAB-IBDC. So far, cooling method for the prototypes of DAB-IBDC is mainly air cooling, and the hardware structures are usually three types: flat and integrate, stereo and integrate, and modular and plug & play, such as the prototype in [110] and [111] and the first prototype in [112] are the flat and integrate structure, the second and third prototypes in [112] and the prototype in [55] are stereo and integrate structure, the prototypes in [99] and [103] are modular and plug & play structure. Fig. 16 gives photos of the different prototypes.
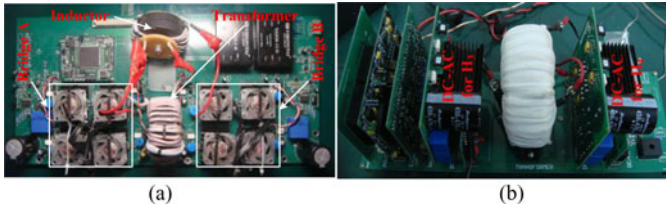
Fig. 16.   Prototypes of DAB-IBDC. (a) Flat and integrate structure. (b) Modular and plug & play structure.
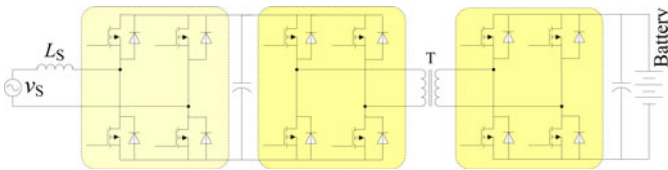

Fig. 17.   HFL BESS based on DAB-IBDC.

In fact, the flat versus stereo structures usually depends on specific cooling conditions, which also further concerns the specific application situation. But compared with the integrate structure, the modular structure can provide plug & play capability and possible high-level fault tolerance. So the modular and plug & play structure is recommended to increase the power density, flexibility, and reliability of DAB-IBDC, which is suitable for HFL PCSs.

VI. Typical Applications of DAB-IBDC for HFL PCSs

DAB-IBDC is widely considered as the core circuit for next-generation HFL PCS, which has a broad market prospect. In this section, several typical application schemes of DAB-IBDC for HFL PCSs will be introduced in the worldwide scope.

A. Battery Energy Storage and Uninterruptible Power Supply

Some literatures discussed the applications of DAB-IBDC for battery energy storage system (BESS) [114], [115], as shown in Fig. 17. BESS adopts DAB-IBDC instead of the traditional buck/boost circuit and line-frequency transformer, so the high-power-density, high-efficiency and high-power-transfer capability can be achieved [114]. The cascaded BESS based on DAB-IBDC to access high-voltage grid was also proposed in [114] and [115].

A multifunctional modular intelligent uninterruptible power supply (IUPS) system based on DAB-IBDC was proposed in [116], as shown in Fig. 18. The IUPS is composed of four identical H-bridge converters, which not only can realize all basic functions of traditional UPS, but also can realize the cyclic use of the electrical power between the power grid and storage battery, it also has an application prospect for LV power distribution of intelligent house in smart grid. Similar to BESS and IUPS applications, DAB-IBDC applications for automotive, electric and hybrid vehicles, as well as renewable energy were also discussed [117]–[120].

However, due to the battery voltage is always changed with the charging and discharging process; HV dc voltages, for this type of applications, must be controlled with the battery voltage in such a way as to minimize the power circulation and loss.
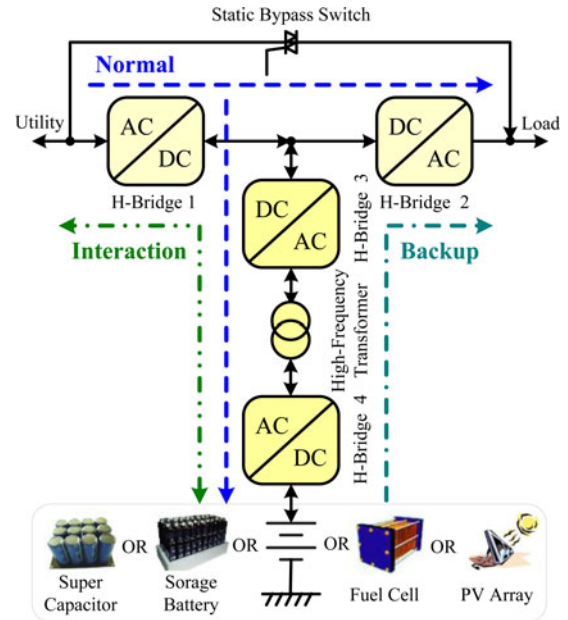

Fig. 18.   HFL IUPS based on DAB-IBDC.

B. Solid-State Transformer (SST)

Literatures [121]–[128] proposed SST as a key device for future renewable electric energy delivery and management system. The topology of SST is shown in Fig. 19(a). It utilizes multilevel topology and traditional dc–ac inverter to handle the 7.2-kV ac input voltage and 120 /240-V ac output voltage, respectively. Additionally, DAB-IBDC was proposed as an everlasting key component to interface between HV and LV dc buses. SST not only can act as a replacement for the traditional distribution transformer, but also can provide functions of voltage sag restoration, power factor correction, and fault current limiting. Compared with traditional distribution transformer, SST reduces the volume and weight of DAB-IBDC. On this basis, some studies also discussed distributed grid and microgrid solution schemes based on SST [129]–[133]. Except these, the SST technology for traction application was discussed comprehensively in [134].

In Fig. 19(a), SST mainly targets the ac transformer. Based on SST concept, the dc transformer based on DAB-IBDC was also analyzed in [135] and [136], as shown in Fig. 19(b). The DAB-IBDCs in the dc transformer are connected in input-series-output-parallel structure, which enables the use of low-voltage (LV) switches, and features low conduction loss and good switching performance with high-frequency operation, to address medium-voltage input. The DAB-IBDCs in [137]–[139] employ a dual-half-bridge stucture to reduce power loss and cost. And in [140], a compact, high-voltage dc–dc SST based on a series connection of SiC JFETS and one MOSFET in cascode connection in high-voltage switches.

C. Back-to-Back (BTB) System

Literatures [30], [141] proposed a 6.6-kV modular multilevel cascaded BTB system characterized by the use of multiple DAB-IBDCs, as shown in Fig. 20. Two sets of modular
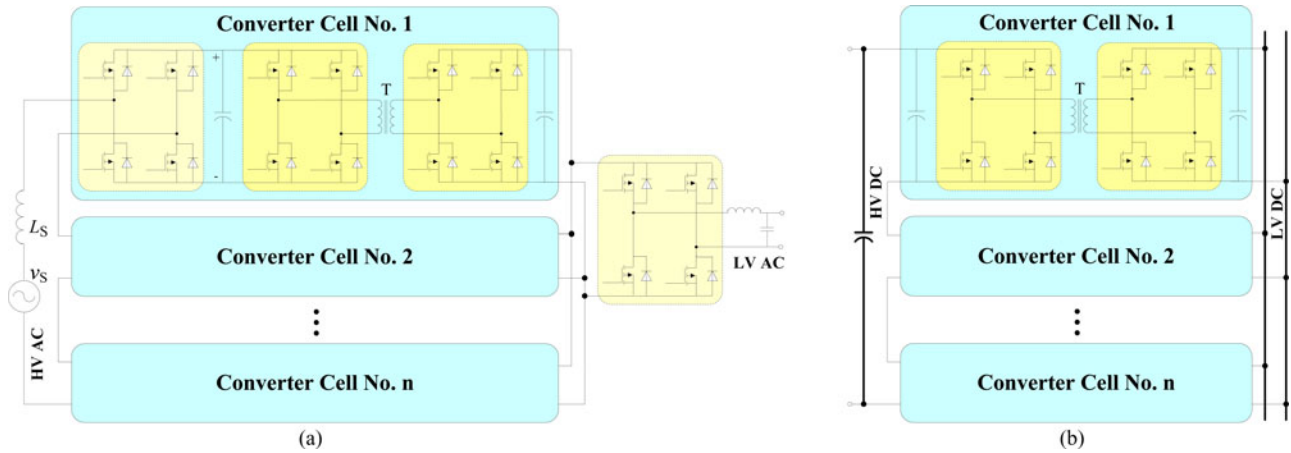
Fig. 19.   (a) HPL ac-ac SST based on DAB-IBDC. (b) HPL dc-dc SST based on DAB-IBDC.
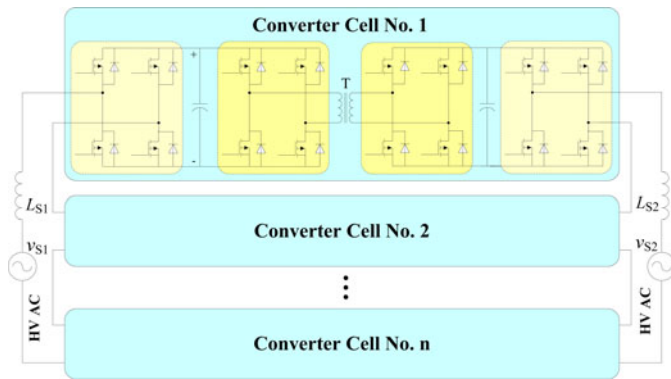

Fig. 20.   HFL BTB system based on DAB-IBDC.

cascaded PWM converters with low-voltage steps make a significant contribution to mitigating supply harmonic currents and EMI emissions [141]. In addition, the employ of DAB-IBDC not only provides the galvanic isolation between the two feeders, but also decreases the volume and weight of the system and resulting in no circulating zero-sequence current.

BTB system is also the key device in a universal flexible power management project [142], [143], which is to develop advanced power conversion technique to meet the future needs of electricity network in Europe. In [144], the BTB system is also used for medium-voltage motor drive applications.

VII. Design Recommendations and Future Trends

A. Design Recommendations

According to the previous analysis, the general design procedure and recommendations for DAB-IBDC in HFL PCSs are shown in Fig. 21. The design procedure is given that the choice of the topology is the first step, the optimization of the control method is the second step, the design of the parameters is the third step, the choice of the power devices is the fourth step, the design of the magnetic components is the fifth step, and the optimization of the hardware structure is the last step.

From the analysis in Section I, the most widely used converter in the HFL PCSs is still the typical DAB IBDC in Fig. 2. So

here takes DAB-IBDC for BESS as an example to introduce the design recommendations.

In control methods of DAB-IBDC, TPS control is the most difficult to implement, and there is also not a unified implement standard at present. In EPS control, the operating states of the two bridges should be changed when the voltage conversion states or the power flow directions are changed. In SPS control, efficiency, ZVS range, etc., have flaws. So in the engineering applications, the DPS control may be the relative optimal method from the implementation difficulty and performance.

In parameter design, the input and output voltages V_1 and V_2, transformer turn ratio n, auxiliary inductance L (included transformer leakage inductance), and switching frequency f_s are the main parameters that should be determined. Usually, the input and output voltages are determined by the specific applications. For instance, in the BESS discussed in Section VI, the input voltage is controlled by the bidirectional dc–ac converter, in order to reduce harmonics and improve power factor, the dc voltage for the dc–ac converter that connect to the 220-V/50-Hz ac grid is usually restricted to 350–450 V, and the standard value is 380 or 400 V [145]. Output voltage is determined by the used storage battery system, which is usually made up of a series of 6- or 12-V cells, and the standard values are 48, 192, 240 V, etc. The transformer turn ratio n should match the voltage conversion ratio of DAB-IBDC to decrease circulating current and increase efficiency. Hence, in an actual system, the input and output voltage levels and transformer turn ratio are usually determined by specific applications.

Auxiliary inductance L and switching frequency f_s have a direct impact on the transmission power, peak current, and RMS current of DAB-IBDC. In order to ensure safe and reliable operation, the design of L and f_s must satisfy the following requirements: 1) transmission power can achieve the required maximum power of load; 2) current stress of the components remains throughout in a bearable range; and 3) current RMS values of the components remain throughout in a bearable range. In addition, the design of L and f_s must consider optimizing of the efficiency and power density.

In choosing power devices, WBG power devices are recommended to improve the efficiency and power density, especially
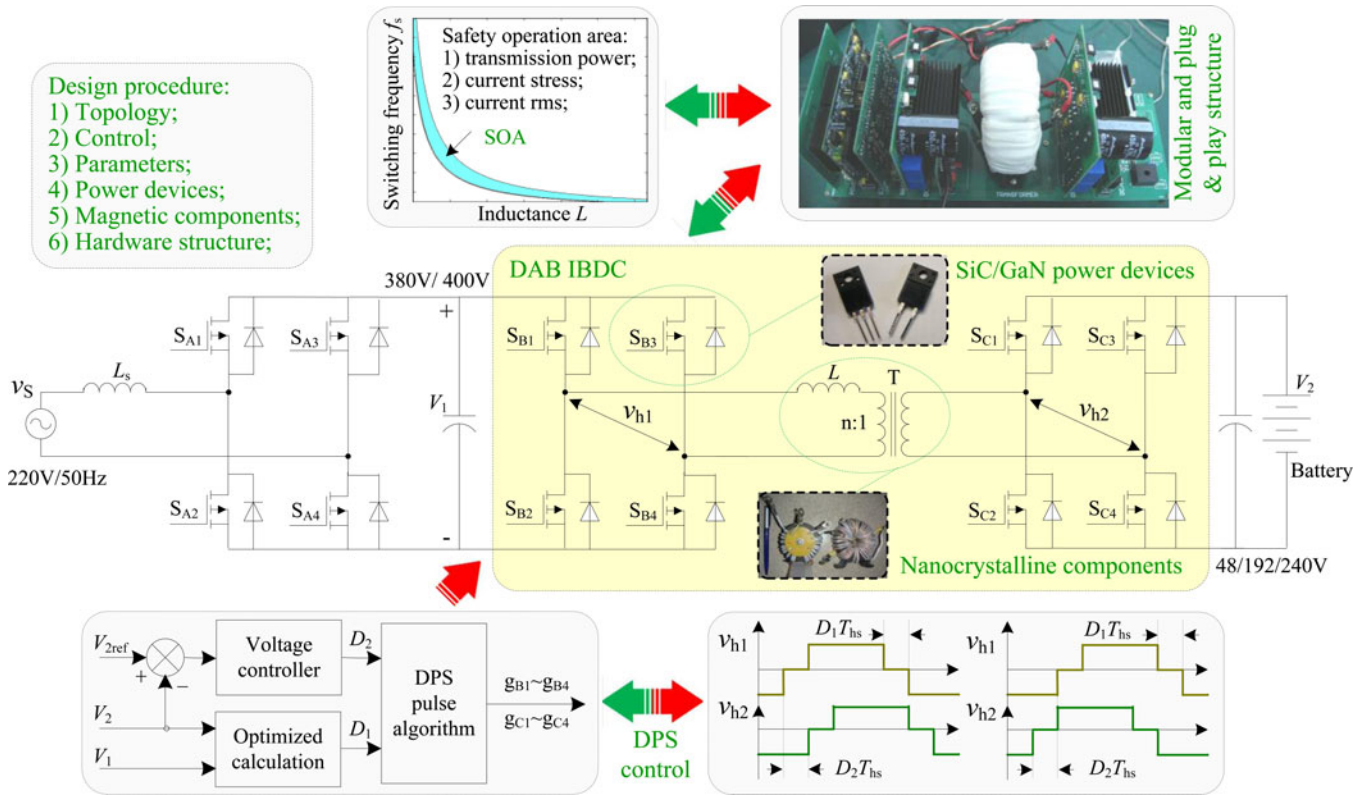
Fig. 21.   General design procedure and recommendations for IBDC in HFL PCSs.

in HFL PCS. And the SiC/GaN power devices may be the key to solve the application bottlenecks of HF IBDC.

In designing the magnetic components, the iron-based nanocrystalline material is recommended to improve the efficiency and power density.

In designing the hardware structure, integrating the auxiliary inductor and transformer into a single module is a recommended approach, and the modular and plug & play hardware structure is recommended to increase the power density, flexibility, and reliability of DAB-IBDC.

B. Future Trends

In view of the research status of DAB-IBDC aforementioned, so far, many researches in the world have focused on the basic characterization, topology and soft-switching solution, control strategy, and hardware design and optimization.

In future, design and performance optimization of DAB-IBDC based on SiC/GaN power devices, and the system-level solutions of DAB-IBDC for HFL PCSs will be the trend, and further key issues may be : 1) the electrical optimization design methods of the topology, electrical parameters, and control strategy of DAB-IBDC based on SiC/GaN power devices to fully utilize their high-temperature, high-frequency, and low-loss characteristics; 2) the mechanical optimization design methods of DAB-IBDC based on SiC/GaN power devices to further improve efficiency, power density, modularity, and reliability of HFL PCSs; 3) the multifunctional, modular, and intelligent HFL PCS solution with high-efficiency and high-power-density, which uses DAB-IBDC as the core circuit; and 4) the intelli-

gent power, voltage, and fault control management methods of intelligent HFL PCS based on DAB-IBDC.

VIII. CONCLUSION

DAB-IBDC is widely considered as the core circuit for next-generation HFL PCSs, which have a broad market prospect. This paper reviewed the current research status of DAB-IBDC. The development history and research necessity of DAB-IBDC were introduced, and the research subjects about the basic characterization, control strategy, soft-switching solution and variant, as well as hardware design and optimization were reviewed and analyzed comprehensively. On this basis, several typical application schemes of DAB-IBDC for HPL PCSs were given in a worldwide scope. In addition, some design recommendations and future trends were presented in this paper. With recent advances in solid-state semiconductors, magnetic and capacitive materials, and microelectronic technologies, the large-scale practical use of DAB-IBDC for HFL PCSs is expected. And in the future, the design and performance optimization of DAB-IBDC based on advanced power devices, and the system-level solutions of DAB-IBDC for HFL PCSs will be the trend.

REFERENCES

[1] J. C. Wu and H. L. Jou, "A new UPS scheme provides harmonic suppression and input power factor correction," *IEEE Trans. Ind. Electron.*, vol. 42, no. 6, pp. 629–635, Dec. 1995.
[2] P. K. Jain, J. R. Espinoza, and H. Jin, "Performance of a single-stage UPS system for single-phase trapezoidal-shaped ac-voltage supplies," *IEEE Trans. Power Electron.*, vol. 13, no. 5, pp. 912–923, Sep. 1998.

[3] J. RodrÍguez, S. Bernet, B. Wu, J. O. Pontt, and S. Kouro, "Multi-level voltage-source-converter topologies for industrial medium-voltage drives," *IEEE Trans. Ind. Electron.*, vol. 54, no. 6, pp. 2930–2945, Dec. 2007.

[4] S. Roy and L. Umanand, "Integrated magnetics-based multisource quality ac power supply," *IEEE Trans. Ind. Electron.*, vol. 58, no. 4, pp. 1350–1358, Apr. 2011.

[5] G. Franceschini, E. Lorenzani, and G. Buticchi, "Saturation compensation strategy for grid connected converters based on line frequency transformers," *IEEE Trans. Energy Convers.*, vol. 27, no. 2, pp. 229–237, Jun. 2012.

[6] D. Sha, G. Xu, and X. Z. Liao, "Control strategy for input-series-output-series high-frequency ac-link inverters," *IEEE Trans. Power Electron.*, vol. 28, no. 11, pp. 5283–5292, Nov. 2013.

[7] R. Huang and S. K. Mazumder, "A soft-switching scheme for an isolated dc/dc converter with pulsating dc output for a three-phase high-frequency-link PWM converter," *IEEE Trans. Power Electron.*, vol. 24, no. 10, pp. 2276–2288, Oct. 2009.

[8] L. Jia and S. K. Mazumder, "A loss-mitigating scheme for dc/pulsating-dc converter of a high-frequency-link system," *IEEE Trans. Ind. Electron*, vol. 59, no. 12, pp. 4537–4544, Dec. 2012.

[9] S. K. Mazumder and A. K. Rathore, "Primary-side-converter-assisted soft-switching scheme for an ac/ac converter in a cycloconverter-type high-frequency-link inverter," *IEEE Trans. Ind. Electron*, vol. 58, no. 9, pp. 4161–4166, Sep. 2011.

[10] J. S. Lai and D. J. Nelson, "Energy management power converters in hybrid electric and fuel cell vehicles," *Proc. IEEE.*, vol. 95, no. 4, pp. 766–777, Apr. 2007.

[11] H. S. H. Chung, W. L. Cheung, and K. S. Tang, "A ZCS bidirectional flyback dc/dc converter," *IEEE Trans. Power Electron.*, vol. 19, no. 6, pp. 1426–1434, Nov. 2004.

[12] M. Kashif, "Bidirectional flyback dc-dc converter for hybrid electric vehicle: Utility, working and PSPICE computer model," in *Proc. Asia Pacific Conf. Postgraduate Res. Microelectron. Electron.*, 2012, pp. 61–66.

[13] A. A. Aboulnaga and A. Emadi, "Performance evaluation of the isolated bidirectional Cuk converter with integrated magnetics," in *Proc. 35th IEEE Annu. Power Electron. Spec. Conf.*, 2004, pp. 1557–1562.

[14] D. M. Bellur and M. K. Kazimierczuk, "Isolated two-transistor zeta converter with reduced transistor voltage," *IEEE Trans. Circuits Syst. II: Exp. Briefs.*, vol. 58, no. 1, pp. 41–45, Jan. 2011.

[15] F. Zhang and Y. Yan, "Novel forward-flyback hybrid bidirectional dc-dc converter," *IEEE Trans. Ind. Electron.*, vol. 56, no. 5, pp. 1578–1584, May 2009.

[16] H. Xiao and S. Xie, "A ZVS bidirectional dc-dc converter with phase-shift plus PWM control scheme," *IEEE Trans. Power Electron.*, vol. 23, no. 2, pp. 813–823, Mar. 2008.

[17] Z. Zhang, O. C. Thomsen, and M. A. E. Andersen, "Optimal design of a push-pull-forward half-bridge (PPFHB) bidirectional dc-dc converter with variable input voltage," *IEEE Trans. Ind. Electron.*, vol. 59, no. 7, pp. 2761–2771, Jul. 2012.

[18] E. V. Souza and I. Barbi, "Bidirectional current-fed flyback-push-pull dc-dc converter," in *Proc. Brazilian Power Electron. Conf.*, 2011, pp. 8–13.

[19] H. Li, F. Z. Peng, and J. S. Lawler, "A natural ZVS medium-power bidirectional dc-dc converter with minimum number of devices," *IEEE Trans. Ind. Appl.*, vol. 39, no. 2, pp. 525–535, Mar./Apr. 2003.

[20] F. Z. Peng, H. Li, G. J. Su, and J. S. Lawler, "A new ZVS bidirectional dc-dc converter for fuel cell and battery application," *IEEE Trans. Power Electron.*, vol. 19, no. 1, pp. 54–65, Jan. 2004.

[21] Z. Zhang, Z. Ouyang, O. C. Thomesen, and M. A. E. Andersen, "Analysis and design of a bidirectional isolated dc-dc converter for fuel cells and supercapacitors hybrid system," *IEEE Trans. Power Electron.*, vol. 27, no. 2, pp. 848–859, Feb. 2012.

[22] J. Y. Lee, Y. S. Jeong, and B. M. Han, "A two-stage isolated bidirectional dc/dc converter with current ripple reduction technique," *IEEE Trans. Ind. Electron.*, vol. 59, no. 1, pp. 644–646, Jan. 2012.

[23] D. Xu, C. Zhao, and H. Fan, "A PWM plus phase-shift control bidirectional dc-dc converter," *IEEE Trans. Power Electron.*, vol. 19, no. 3, pp. 666–675, May 2004.

[24] H. J. Chiu and L. W. Lin, "A bidirectional dc-dc converter for fuel cell electric vehicle driving system," *IEEE Trans. Power Electron.*, vol. 21, no. 4, pp. 950–958, Jul. 2006.

[25] L. Roggia, L. Schuch, J. E. Baggio, C. Rech, and J. R. Pinheiro, "Integrated full-bridge-forward dc-dc converter for a residential microgrid application," *IEEE Trans. Power Electron.*, vol. 28, no. 4, pp. 1728–1740, Apr. 2013.

[26] K. Wang, C. Y. Lin, L. Zhu, D. Qu, F. C. Lee, and J. S. Lai, "Bidirectional dc to dc converters for fuel cell systems," in *Proc. Power Electron. Transp.*, 1998, pp. 47–51.

[27] T. Hirose and H. Matsuo, "A consideration of bidirectional superposed dual active bridge dc-dc converter," in *Proc. 2nd IEEE Int. Symp. Power Electron. Distrib. Generation Syst.*, 2010, pp. 39–46.

[28] B. Zhao, Q. Yu, Z. Leng, and X. Chen, "Switched Z-source isolated bidirectional dc-dc converter and its phase-shifting shoot through bivariate coordinated control strategy," *IEEE Trans. Ind. Electron.*, vol. 59, no. 12, pp. 4657–4670, Dec. 2012.

[29] L. Zhu, "A novel soft-commutating isolated boost full-bridge ZVS-PWM dc-dc converter for bidirectional high power applications," *IEEE Trans. Power Electron.*, vol. 21, no. 2, pp. 422–429, Mar. 2006.

[30] S. Inoue and H. Akagi, "A bidirectional isolated dc-dc converter as a core circuit of the next-generation medium-voltage power conversion system," *IEEE Trans. Power Electron.*, vol. 22, no. 2, pp. 535–542, Mar. 2007.

[31] S. Inoue and H. Akagi, "A bidirectional dc-dc converter for an energy storage system with galvanic isolation," *IEEE Trans. Power Electron.*, vol. 22, no. 6, pp. 2299–2306, Nov. 2007.

[32] R. W. A. A. D. Doncker, D. M. Divan, and M. H. Kheraluwala, "A three-phase soft-switched high-power-density dc/dc converter for high-power applications," *IEEE Trans. Ind. Appl.*, vol. 27, no. 1, pp. 63–73, Jan./Feb. 1991.

[33] M. H. Kheraluwala, R. W. Gascoigne, D. M. Divan, and E. D. Baumann, "Performance characterization of a high-power dual active bridge dc-to-dc converter," *IEEE Trans. Ind. Appl.*, vol. 28, no. 6, pp. 1294–1301, Nov./Dec. 1992.

[34] M. H. Kheraluwala and R. W. D. Doncker, "Single phase unity power factor control for dual active bridge converter," in *Proc. IEEE Ind. Appl. Soc. Annu. Meet.*, 1993, pp. 909–916.

[35] H. L. Chan, K. W. E. Cheng, and D. Sutanto, "A novel square-wave converter with bidirectional power flow," in *Proc. IEEE Int. Conf. Power Electron. Drive Syst.*, 1999, pp. 966–971.

[36] H. L. Chan, K. W. E. Cheng, and D. Sutanto, "Phase-shift controlled dc-dc converter with bidirectional power flow," *IEE Proc. Electric Power Appl.*, vol. 148, no. 2, pp. 193–201, Mar. 2001.

[37] H. L. Chan, K. W. E. Cheng, and D. Sutanto, "ZCS-ZVS bidirectional phase-shifted dc-dc converter with extended load range," *IEE Proc. Electric Power Appl.*, vol. 150, no. 3, pp. 269–277, May 2003.

[38] J. Biela, M. Schweizer, S. Waffler, and J. W. Kolar, "SiC versus Si-Evaluation of potentials for performance improvement of inverter and dc-dc converter systems by SiC power semiconductors," *IEEE Trans. Ind. Electron.*, vol. 58, no. 7, pp. 2872–2882, Jul. 2011.

[39] M. C. Lee, C. Y. Lin, S. H. Wang, and T. S. Chin, "Soft-magnetic Fe-based nano-crystalline thick ribbons," *IEEE Trans. Magn.*, vol. 44, no. 11, pp. 3836–3838, Nov. 2008.

[40] C. Mi, H. Bai, C. Wang, and S. Gargies, "Operation, design and control of dual H-bridge-based isolated bidirectional dc-dc converter," *IET Power Electron.*, vol. 1, no. 4, pp. 507–517, Jul. 2008.

[41] A. R. Alonso, J. Sebastian, D. G. Lamar, M. M. Hernando, and A. Vazquez, "An overall study of a dual active bridge for bidirectional dc/dc conversion," in *Proc. IEEE Energy Convers. Congr. Expo.*, 2010, pp. 1129–1135.

[42] G. G. Oggier, M. Ordonez, J. M. Galvez, and F. Luchino, "Fast transient boundary control and steady-state operation of the dual active bridge converter using the natural switching surface," *IEEE Trans. Power Electron.*, vol. 29, no. 2, pp. 946–957, Feb. 2014.

[43] H. Bai, C. Mi, and S. Gargies, "The short-time-scale transient processes in high-voltage and high-power isolated bidirectional dc-dc converters," *IEEE Trans. Power Electron.*, vol. 23, no. 6, pp. 2648–2656, Nov. 2008.

[44] B. Zhao, Q. Yu, and W. Sun, "Extended-phase-shift control of isolated bidirectional dc-dc converter for power distribution in microgrid," *IEEE Trans. Power Electron.*, vol. 27, no. 11, pp. 4667–4680, Nov. 2012.

[45] B. Zhao, Q. Song, and W. Liu, "Power characterization of isolated bidirectional dual-active-bridge dc-dc converter with dual-phase-shift control," *IEEE Trans. Power Electron.*, vol. 27, no. 9, pp. 4172–4176, Sep. 2012.

[46] H. Bai and C. Mi, "Eliminate reactive power and increase system efficiency of isolated bidirectional dual-active-bridge DC-DC converters using novel dual-phase-shift control," *IEEE Trans. Power Electron.*, vol. 23, no. 6, pp. 2905–2914, Nov. 2008.

[47] Y. Xie, J. Sun, and J. S. Freudenberg, "Power flow characterization of a bidirectional galvanically isolated high-power dc-dc converter over a wide operating range," *IEEE Trans. Power Electron.*, vol. 25, no. 1, pp. 54–66, Jan. 2010.

[48] B. Zhao, Q. Song, W. Liu, and Y. Sun, "Dead-time effect of the high-frequency isolated bidirectional full-bridge dc-dc converter: Comprehensive theoretical analysis and experimental verification," *IEEE Trans. Power Electron.*, vol. 29, no. 4, pp. 1667–1680, Apr. 2014.

[49] J. Li, Z. Chen, Z. Shen *et al.*, "An adaptive dead-time control scheme for high-switching-frequency dual-active-bridge converter," in *Proc. 27th Annu. IEEE Appl. Power Electron. Conf. Expo.*, 2012, pp. 1355–1361.

[50] D. Costinett, R. Zane, and D. Maksimovic, "Automatic voltage and dead time control for efficiency optimization in a dual active bridge converter," in *Proc. 27th Annu. IEEE Appl. Power Electron. Conf. Expo.)*, 2012, pp. 1104–1111.

[51] G. D. Demetriades and H. P. Nee, "Dynamic modeling of the dual-active bridge topology for high-power applications," in *Proc. IEEE Power Electron. Spec. Conf.*, 2008, pp. 457–464.

[52] H. Bai, C. Mi, C. Wang, and S. Gargies, "The dynamic model and hybrid phase-shift control of a dual-active-bridge converter," in *Proc. 34th Annu. Conf. IEEE Ind. Electron. Soc. (IECON)*, 2008, pp. 2840–2845.

[53] H. Bai, Z. Nie, and C. Mi, "Experimental comparision of traditional phase-shift, dual-phase-shift, and model-based control of isolated bidirectional dc-dc converters," *IEEE Trans. Power Electron.*, vol. 25, no. 6, pp. 1444–1449, Jun. 2010.

[54] C. Zhao, S. D. Round, and J. W. Kolar, "Full-order averaging modeling of zero-voltage-switching phase-shift bidirectional dc-dc converters," *IET Power Electron.*, vol. 3, no. 3, pp. 400–410, Apr. 2010.

[55] F. Krismer and J. W. Kolar, "Accurate small-signal model for the digital control of an automotive bidirectional dual active bridge," *IEEE Trans. Power Electron.*, vol. 24, no. 12, pp. 2756–2768, Dec. 2009.

[56] H. Qin and J. W. Kimball, "Generalized average modeling of dual active bridge dc-dc converter," *IEEE Trans. Power Electron.*, vol. 27, no. 4, pp. 2078–2084, Apr. 2012.

[57] D. Costinett, D. Maksimovic, and R. Zane, "Design and control for high efficiency in high step-down dual active bridge converters operating at high switching frequency," *IEEE Trans. Power Electron.*, vol. 28, no. 8, pp. 3931–3940, Aug. 2013.

[58] G. G. Oggier, R. Ledhold, G. O. Garcia, A. R. Oliva, J. C. Balda, and F. Barlow, "Extending the ZVS operating range of dual active bridge high-power dc-dc converters," in *Proc. IEEE Power Electron. Spec. Conf.*, 2006, pp. 1–7.

[59] G. D. Demetriades and H. P. Nee, "Characterization of the dual-active bridge topology for high-power applications employing a duty-cycle modulation," in *Proc. IEEE Power Electron. Spec. Conf.*, 2008, pp. 2791–2798.

[60] G. G. Oggier, G. O. Garcia, and A. R. Oliva, "Switching control strategy to minimize dual active bridge converter losses," *IEEE Trans. Power Electron.*, vol. 24, no. 7, pp. 1826–1838, Jul. 2009.

[61] G. G. Oggier, G. O. Garcia, and A. R. Oliva, "Modulation strategy to operate the dual active bridge dc-dc converter under soft switching in the whole operating range," *IEEE Trans. Power Electron.*, vol. 26, no. 4, pp. 1228–1236, Apr. 2011.

[62] M. Kim, M. Rosekeit, S. K. Sul, and R. W. A. D. Doncker, "A dual-phase –shift control strategy for dual-active-bridge dc-dc converter in wide voltage range," in *Proc. 8th IEEE Int. Conf. Power Electron. ECCE Asia*, 2011, pp. 364–371.

[63] B. Zhao, Q. Song, W. Liu, and W. Sun, "Current-stress-optimized switching strategy of isolated bidirectional dc-dc converter with dual- phase-shift control," *IEEE Trans. Ind. Electron.*, vol. 60, no. 10, pp. 4458–4467, Oct. 2013.

[64] B. Zhao, Q. Song, and W. Liu, "Efficiency characterization and optimization of isolated bidirectional dc-dc converter based on dual- phase-shift control for dc distribution application," *IEEE Trans. Power Electron.*, vol. 28, no. 4, pp. 1711–1727, Apr. 2013.

[65] F. Krismer and J. W. Kolar, "Closed form solution for minimum conduction loss modulation of DAB converters," *IEEE Trans. Power Electron.*, vol. 27, no. 1, pp. 174–188, Jan. 2012.

[66] F. Krismer and J. W. Kolar, "Efficiency-optimized high-current dual active bridge converter for automotive applications," *IEEE Trans. Ind. Electron.*, vol. 59, no. 7, pp. 2745–2760, Jul. 2012.

[67] H. Zhou and A. M. Khambadkone, "Hybrid modulation for dual-active-bridge bidirectional converter with extended power range for ultracapac-itor application," *IEEE Trans. Ind. Appl.*, vol. 45, no. 4, pp. 1434–1442, Jul./Aug. 2009.

[68] Y. Du, S. M. Lukic, B. S. Jacobson, and A. Q. Huang, "Modulation technique to reverse power flow for the isolated series resonant dc-dc converter with clamped capacitor voltage," *IEEE Trans. Ind. Electron.*, vol. 59, no. 12, pp. 4617–4628, Dec. 2012.

[69] K. Wu, C. W. Silva, and W. G. Dunford, "Stability analysis of isolated bidirectional dual active full-bridge dc-dc converter with triple phase-shift control," *IEEE Trans. Power Electron.*, vol. 27, no. 4, pp. 2007–2017, Apr. 2012.

[70] A. K. Jain and R. Ayyanar, "PWM control of dual active bridge: Comprehensive analysis and experimental verification," *IEEE Trans. Power Electron.*, vol. 26, no. 4, pp. 1215–1227, Apr. 2011.

[71] F. Krismer, J. Biela, and J. W. Kolar, "A comparative evaluation of isolated bidirectional dc/dc converters with wide input and output voltage range," in *Proc. 40th Annu. Conf. IEEE Ind. Appl. Soc.*, 2005, pp. 599–606.

[72] H. R. Karshenas, H. Daneshpajooh, A. Safaee, A. Bakhshai, and P. Jain, "Basic families of medium-power soft-switched isolated bidirectional dc-dc converters," in *Proc. 2nd Power Electron., Drive Syst. Technol. Conf.*, 2011, pp. 92–97.

[73] G. Guidi, A. Kawamura, Y. Sasaki, and T. Imakubo, "Dual active bridge modulation with complete zero voltage switching taking resonant transitions into account," in *Proc. 14th Eur. Conf. Power Electron. Appl.*, 2011, pp. 1–10.

[74] X. Li and A. K. S. Bhat, "Analysis and design of high-frequency isolated dual-bridge series resonant dc/dc converter," *IEEE Trans. Power Electron.*, vol. 25, no. 4, pp. 850–862, Apr. 2010.

[75] W. Chen, P. Rong, and Z. Y. Lu, "Snubberless bidirectional DC-DC converter with new CLLC resonant tank featuring minimized switching loss," *IEEE Trans. Ind. Electron.*, vol. 57, no. 9, pp. 3075–3086, Sep. 2010.

[76] J. H. Jung, H. S. Kim, M. H. Ryu, and J. W. Baek, "Design methodology of bidirectional CLLC resonant converter for high-frequency isolation of dc distribution systems," *IEEE Trans. Power Electron.*, vol. 28, no. 4, pp. 1741–1755, Apr. 2013.

[77] W. Chen and Z. Lu, "Investigation on topology for type-4 LLC resonant dc-dc converter," in *Proc. IEEE Power Electron. Spec. Conf.*, 2008, pp. 1421–1425.

[78] S. Jalbrzykowski, A. Bogdan, and T. Citko, "A dual full-bridge resonant class-E bidirectional dc-dc converter," *IEEE Trans. Ind. Electron.*, vol. 58, no. 9, pp. 3879–3883, Sep. 2011.

[79] S. Jalbrzykowski and T. Citko, "Current-fed resonant full-bridge boost dc/ac/dc converter," *IEEE Trans. Ind. Electron.*, vol. 55, no. 3, pp. 1198–1205, Mar. 2008.

[80] A. Rufer and P. Barrade, "A supercapacitor-based energy-storage system for elevators with soft commutated interface," *IEEE Trans. Ind. Appl.*, vol. 38, no. 5, pp. 1151–1159, Sep./Oct. 2002.

[81] D. Chen, "Novel current-mode ac/ac converters with high-frequency ac link," *IEEE Trans. Ind. Electron.*, vol. 55, no. 1, pp. 30–37, Jan. 2008.

[82] D. Chen and Y. Chen, "Step-up ac voltage regulators with high-frequency link," *IEEE Trans. Power Electron.*, vol. 28, no. 1, pp. 390–397, Jan. 2013.

[83] L. Li and Q. Zhong, "Comparisons of two kinds of ac/ac converters with high frequency link," in *Proc. 34th IEEE Annu. Conf. Ind. Electron. Soc.*, 2008, pp. 618–622.

[84] H. Qin and J. W. Kimball, "Ac-ac dual active bridge converter for solid state transformer," in *Proc. IEEE Energy Convers. Congr. Expo.*, 2009, pp. 3039–3044.

[85] H. Qin and J. W. Kimball, "Solid state transformer architecture using ac-ac dual active bridge converter," *IEEE Trans. Ind. Electron.*, vol. 60, no. 9, pp. 3720–3730, Sep. 2012.

[86] J. Walter and R. W. D. Doncker, "High-power galvanically isolated dc/dc converter topology for future automobiles," in *Proc. 34th IEEE Annu. Power Electron. Spec. Conf.*, 2003, pp. 27–32.

[87] D. Segaran, D. G. Holmes, and B. P. Mcgrath, "Comparative analysis of single and three-phase dual active bridge bidirectional dc-dc converters," in *Proc. Australasian Universities Power Eng. Conf.*, 2008, pp. 1–6.

[88] N. Soltau, H. A. B. Siddique, and R. W. D. Doncker, "Comparehensive modeling and control strategies for a three-phase dual-active-bridge," in *Proc. Int. Conf. Renewable Energy Res. Appl.*, 2012, pp. 1–6.

[89] S. P. Engel, N. Soltau, H. Stagge, and R. W. D. Doncker, "Dynamic and balanced control of three-phase high-power dual-active bridge dc-dc

converters in dc-grid applications," *IEEE Trans. Power Electron.*, vol. 28, no. 4, pp. 1880–1889, Apr. 2013.

[90] H. Hoek, M. Neubert, and R. W. D. Doncker, "Enhanced modulation strategy for a three-phase dual active bridge—boosting efficiency of an electric vehicle converter," *IEEE Trans. Power Electron.*, vol. 28, no. 12, pp. 5499–5507, Dec. 2013.

[91] H. Tao, A. Kotsopoulos, J. L. Duarte, and M. A. M. Hendrix, "A soft-switched three-port bidirectional converter for fuel cell and supercapacitor applications," in *Proc. 36th IEEE Power Electron. Spec. Conf.*, 2005, pp. 2487–2493.

[92] H. Tao, A. Kotsopoulos, J. L. Duarte, and M. A. M. Hendrix, "Design of a soft-switched three-port converter with DSP control for power flow management in hybrid fuel cell systems," in *Proc. Eur. Conf. Power Electron. Appl.*, 2005, pp. 1–10.

[93] H. Tao, A. Kotsopoulos, J. L. Duarte, and M. A. M. Hendrix, "Family of multiport bidirectional dc-dc converters," *IEE Proc. Electric Power Appl.*, vol. 153, no. 3, pp. 451–458, May 2006.

[94] C. Zhao, S. D. Round, and J. W. Kolar, "An isolated three-port bidirectional dc-dc converter with decoupled power flow management," *IEEE Trans. Power Electron.*, vol. 23, no. 5, pp. 2443–2453, Sep. 2008.

[95] H. Tao, A. Kotsopoulos, J. L. Duarte, and M. A. M. Hendrix, "Triple-half- bridge bidirectional converter controlled by phase shift and PWM," in *Proc. 21st IEEE Annu. Appl. Power Electron. Conf. Expo.*, 2006, pp. 1256–1262.

[96] M. Phattanasak, R. G. Ghoachani, J. P. Martin, S. Pierfederici, and B. Davat, "Flatness based control of an isolated three-port bidirectional dc-dc converter for a fuel cell hybrid source," in *Proc. IEEE Energy Convers. Congr. Expo.*, 2011, pp. 977–984.

[97] Z. Wang and H. Li, "An integrated three-port bidirectional dc-dc converter for PV application on a dc distribution system," *IEEE Trans. Power Electron.*, vol. 28, no. 10, pp. 4612–4624, Oct. 2013.

[98] F. Krismer and J. W. Kolar, "Accurate power loss model derivation of a high-current dual active bridge converter for an automotive application," *IEEE Trans. Ind. Electron.*, vol. 57, no. 3, pp. 881–891, Mar. 2010.

[99] B. Zhao, Q. Song, W. Liu, and Y. Sun, "A synthetic discrete design methodology of high-frequency isolated bidirectional dc-dc converter for grid-connected battery energy storage system using advanced components," *IEEE Trans. Ind. Electron.*, early access, 2013.

[100] D. D. V. Ramanarayanan, "Improved utilization of an HF transformer in dc-ac application," *IET Power Electron.*, vol. 4, no. 5, pp. 508–515, May 2011.

[101] H. Qin, J. W. Kimball, and G. K. Venayagamoorthy, "Particle swarm optimization of high-frequency transformer," in *Proc. 36th IEEE Annu. Conf. Ind. Electron. Soc.*, 2010, pp. 2914–2919.

[102] G. Guidi, M. Pavlovsky, A. Kawamura, T. Imakubo, and Y. Sasaki, "Improvement of light load efficiency of dual active bridge dc-dc converter by using dual leakage transformer and variable frequency," in *Proc. IEEE Energy Convers. Congr. Expo.*, 2010, pp. 830–837.

[103] H. Fan and H. Li, "High-frequency transformer isolated bidirectional dc-dc converter modules with high efficiency over wide load range for 20 kVA solid-state transformer," *IEEE Trans. Power Electron.*, vol. 26, no. 12, pp. 3599–3609, Dec. 2011.

[104] G. Guidi, M. Pavlovsky, A. Kawamura, T. Imakubo, and Y. Sasaki, "Efficiency optimization of high power density dual active bridge dc-dc converter," in *Proc. Int. Power Electron. Conf.*, 2010, pp. 981–986.

[105] Y. Du, S. Baek, S. Bhattacharya, and A. Q. Huang, "High-voltage high-frequency transformer design for a 7.2 kV to 120 V/240 V 20 kVA solid state transformer," in *Proc. 36th IEEE Annu. Conf. Ind. Electron. Soc.*, 2010, pp. 493–498.

[106] Y. Wang, S. W. H. Haan, and J. A. Ferreira, "Design of low-profile nanocrystalline transformer in high-current phase-shifted dc-dc converter," in *Proc. IEEE Energy Convers. Congr. Expo.*, 2010, pp. 2177–2181.

[107] D. Aggeler, J. Biela, S. Inoue, H. Akagi, and J. W. Kolar, "Bidirectional isolated dc-dc converter for next-generation power distribution-comparison of converters using Si and SiC devices," in *Proc. Power Convers. Conf.*, 2007, pp. 510–517.

[108] D. Costinett, H. Nguyen, R. Zane, and D. Maksimovic, "GaN-FET based dual active bridge dc-dc converter," in *Proc. 26th IEEE Annu. Appl. Power Electron. Conf. Expo.*, 2011, pp. 1425–1432.

[109] A. Kadavelugu, S. Baek, S. Dutta, S. Bhattacharya, M. Das, A. Agarwal, and J. Scofield, "High-frequency design considerations of dual active bridge 1200 V SiC MOSFET dc-dc converter," in *Proc. 26th IEEE Annu. Appl. Power Electron. Conf. Expo.*, 2011, pp. 314–320.

[110] B. Zhao, Q. Song, W. Liu, and Y. Sun, "Characterization and application of next-generation SiC power devices for high-frequency isolated bidirectional dc-dc converter," in *Proc. 38th IEEE Annu. Conf. Ind. Electron. Soc.*, 2012, pp. 281–286.

[111] B. Zhao, Q. Song, and W. Liu, "Experimental comparison of isolated bidirectional dc-dc converters based on all-Si and All-SiC power devices for next-generation power conversion application," *IEEE Trans. Ind. Electron.*, vol. 61, no. 3, pp. 1389–1393, Mar. 2014.

[112] Y. Wang, S. W. H. Haan, and J. A. Ferreira, "Potential of improving PWM converter power density with advanced components," in *Proc. 13th Eur. Conf. Power Electron. Appl.*, 2009, pp. 1–10.

[113] J. W. Chung, K. Ryu, B. Lu, and T. Palacios, "GaN-on-Si technology, a new approach for advanced devices in energy and communications," in *Proc. Eur. Solid-State Device Res. Conf.*, 2010, pp. 52–56.

[114] N. M. L. Tan, T. Abe, and H. Akagi, "Design and performance of a bidirectional isolated dc-dc converter for a battery energy storage system," *IEEE Trans. Power Electron.*, vol. 27, no. 3, pp. 1237–1248, Mar. 2012.

[115] B. Reese, M. Schupbach, A. Lostetter, B. Rowden, R. Saunders, and J. Balda, "High voltage, high power density bidirectional multi-level converters utilizing silicon and silicon carbide (SiC) switches," in *Proc. 23th IEEE Annu. Appl. Power Electron. Conf. Expo.*, 2008, pp. 252–258.

[116] B. Zhao, Q. Song, W. Liu, and Y. Xiao, "Next-generation multi-functional modular intelligent UPS system for smart grid," *IEEE Trans. Ind. Electron.*, vol. 60, no. 9, pp. 3602–3618, Sep. 2013.

[117] G. J. Su and L. Tang, "A three-phase bidirectional dc-dc converter for automotive applications," in *Proc. IEEE Ind. Appl. Soc. Annu. Meet.*, 2008, pp. 1–7.

[118] J. H. Jung, C. K. Kwon, J. P. Hong, E. C. Nho, H. G. Kim, and T. W. CHun, "Power control and transformer design method of bidirectional dc-dc converter for a hybrid generation system," in *Proc. IEEE Vehicle Power Propulsion Conf.*, 2012, pp. 1512–1515.

[119] H. Qin and J. W. Kimball, "Closed-loop control of dc-dc dual-active-bridge converters driving single-phase inverter," *IEEE Trans. Power Electron.*, vol. 29, no. 2, pp. 1006–1017, Feb. 2014.

[120] H. Krishnaswami and N. Mohan, "Three-port series-resonant dc-dc converter to interface renewable energy sources with bidirectional load and energy storage ports," *IEEE Trans. Power Electron.*, vol. 24, no. 10, pp. 2289–2297, Oct. 2009.

[121] T. Zhao, J. Zeng, S. Bhattacharya, M. E. Baran, and A. Q. Huang, "An average model of solid state transformer for dynamic system simulation," in *Proc. IEEE Power Energy Soc. General Meet.*, 2009, pp. 1–8.

[122] S. Bhattacharya, T. Zhao, G. Wang, S.Dutta, S. Baek, Y. Du, B. Parkhideh, X. Zhou, and A. Q. Huang, "Design and development of Generation-I silicon based solid state transformer," in *Proc. 25th IEEE Annu. Appl. Power Electron. Conf. Expo.*, 2010, pp. 1666–1673.

[123] H. Fan and H. Li, "A novel phase-shift bidirectional dc-dc converter with an extended high-efficiency range for 20 kVA solid state transformer," in *Proc. IEEE Energy Convers. Congr. Expo.*, 2010, pp. 3870–3876.

[124] G. Wang, S. Baek, J. Elliott, A. Kadavelugu, F. Wang, X. She, S. Dutta, Y. Liu, T. Zhao, W. Yao, R. Gould, S. Bhattacharya, and A. Q. Huang, "Design and hardware implementation of Gen-1 silicon based solid state transformer," in *Proc. 26th IEEE Annu. Appl. Power Electron. Conf. Expo.*, 2011, pp. 1344–1349.

[125] H. Wang, X. Tan, Q. Li, F. Zhou, Z. Deng, Z. Li, and N. Lu, "Development and applicability analysis of intelligent solid state transformer," in *Proc. 4th Int. Conf. Electric Utility Deregulat. Restruct. Power Technol.*, 2011, pp. 1150–1154.

[126] A. Q. Huang, M. L. Crow, G. T. Heydt, J. P. Zheng, and S. J. Dale, "The future renewable electric energy delivery and management (FREEDM) system: The energy internet," *Proc. IEEE.*, vol. 99, no. 1, pp. 133–148, Jan. 2011.

[127] J. Shi, W. Gou, H. Yuan *et al.*, "Research on voltage and power balance control for cascaded modular solid-state transformer," *IEEE Trans. Power Electron.*, vol. 26, no. 4, pp. 1154–1166, Apr. 2011.

[128] X. She, A. Q. Huang, and G. Wang, "3-D space modulation with voltage balancing capability for a cascaded seven-level converter in a solid-state transformer," *IEEE Trans. Power Electron.*, vol. 26, no. 12, pp. 3778–3789, Dec. 2011.

[129] K. Stefanski, H. Qin, B. H. Chowdhury, J. W. Kimball, and S. Bhattacharya, "Identifying techniques, topologies and features for maximizing the efficiency of a distribution grid with solid state power devices," in *Proc. North Am. Power Symp.*, 2010, pp. 1–7.

[130] F. Wang, X. Lu, W. Wang, A. Q. Huang *et al.*, "Development of distributed grid intelligence platform for solid state transformer," in *Proc. IEEE Int. Conf. Smart Grid Commun.*, 2012, pp. 481–485.

[131] X. She, R. Burgos, G. Wang, F. Wang, and A. Q. Huang, "Review of solid state transformer in the distribution system: from components to field application," in *Proc. IEEE Energy Convers. Congr. Expo.*, 2012, pp. 4077–4084.

[132] X. She, S. Lukic, A. Q. Huang, S. Bhattacharya, and M. Baran, "Performance evaluation of solid state transformer based microgrid in FREEDM systems," in *Proc. 26th IEEE Annu. Appl. Power Electron. Conf. Expo.*, 2011, pp. 182–188.

[133] X. She, A. Q. Huang, S. Lukic, and M. E. Baran, "On integration of solid- state transformer with zonal dc microgrid," *IEEE Trans. Smart Grid.*, vol. 3, no. 2, pp. 975–985, Jun. 2012.

[134] D. Dujic, F. Kieferndorf, C. Francisco, and U. Drofenik, "Power electronic traction transformer technology," in *Proc. Int. Power Electron. Motion Control Conf.*, 2012, pp. 636–642.

[135] G. Ortiz, J. Biela, D. Bortis, and J. W. Kolar, "1 megawatt, 20 kHz, isolated, bidirectional 12 kV to 1.2 kV dc-dc converter for renewable energy applications," in *Proc. Int. Power Electron. Conf.*, 2010, pp. 3212–3219.

[136] M. Rashed, C. Klumpner, and G. Asher, "High performance multilevel converter topology for interfacing energy storage systems with medium voltage grids," in *Proc. 36th IEEE Annu. Conf. Ind. Electron. Soc.*, 2010, pp. 1825–1831.

[137] H. Fan and H. Li, "High frequency high efficiency bidirectional dc-dc converter module design for 10 kVA solid state transformer," in *Proc. 25th IEEE Annu. Appl. Power Electron. Conf. Expo.*, 2010, pp. 210–215.

[138] H. Fan and H. Li, "A distributed control of input-series-output-parallel bidirectional dc-dc converter modules applied for 20 kVA solid state transformer," in *Proc. 26th IEEE Annu. Appl. Power Electron. Conf. Expo.*, 2011, pp. 939–945.

[139] H. Fan and H. Li, "A high-frequency medium-voltage dc-dc converter for future electric energy delivery and management systems," in *Proc. 8th IEEE Int. Conf. Power Electron. ECCE Asia*, 2011, pp. 1031–1038.

[140] D. Aggeler, J. Biela, and J. W. Kolar, "A compact, high voltage 25 kW, 50 kHz dc-dc converter based on SiC JFETs," in *Proc. 23th IEEE Annu. Appl. Power Electron. Conf. Expo.*, 2008, pp. 801–807.

[141] H. Akagi and R. Kitada, "Control and design of a modular multilevel cascade BTB system using bidirectional isolated dc/dc converter," *IEEE Trans. Power Electron.*, vol. 26, no. 9, pp. 2457–2464, Sep. 2011.

[142] A. Masoud, P. Wheeler, and J. Chare, "Sliding mode observer design for universal flexible power management (Uniflex-PM) structure," in *Proc. 34th IEEE Annu. Conf. Ind. Electron. Soc.*, 2008, pp. 3321–3326.

[143] S. Bifaretti, P. Zanchetta, A. Watson, L. Tarisciotti, and J. C. Clare, "Advanced power electronic conversion and control system for universal and flexible power management," *IEEE Trans. Smart Grid.*, vol. 2, no. 2, pp. 231–243, Jun. 2011.

[144] S. Inoue and H. Akagi, "Voltage control of a bidirectional isolated dc/dc converter for medium-voltage motor drives," in *Proc. Power Convers. Conf.*, 2007, pp. 1244–1250.

[145] A. Stupar, T. Friedli, J. Miniböck, and J. W. Kolar, "Towards a 99% efficiency three-phase buck-type PFC rectifier for 400-V dc distribution systems," *IEEE Trans. Power Electron.*, vol. 27, no. 4, pp. 1732–1744, Apr. 2012.

Qiang Song (M'12) was born in Changchun, China in 1975. He received the B.S. and Ph.D. degrees from the Department of Electrical Engineering, Tsinghua University, Beijing, China, in 1998 and 2003, respectively.

He is currently an Associate Professor in the Department of Electrical Engineering at Tsinghua University, Beijing, China. His main research interests include high-power electronic interfaces for utility system, flexible ac transmission system and motor drives.
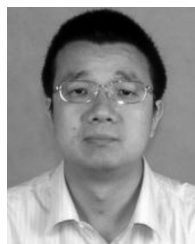
Wenhua Liu (M'03) was born in Hunan, China in 1968. He received the B.S., M.S., and Ph.D. degrees from the Department of Electrical Engineering, Tsinghua University, Beijing, China, in 1988, 1993, and 1996 respectively.

He is currently a Professor in the Department of Electrical Engineering at Tsinghua University, Beijing, China. His main research interests include high-power electronic and flexible ac transmission system.

Yandong Sun was born in Beijing, China in 1962. He graduated from junior college of Beijing University of Posts and Telecommunications, Beijing, China, in 1991.

He is currently an Engineer in the Department of Electrical Engineering at Tsinghua University, Beijing, China. His main research interests include power electronic and power monitoring system.

Biao Zhao (S'11) was born in Hubei, China in 1987. He received the B.S. degree from the Department of Electrical Engineering, Dalian University of Technology, Dalian, China, in 2009. He is currently working toward the Ph.D. degree in the Department of Electrical Engineering, Tsinghua University, Beijing, China.

His current research interests include bidirectional dc–dc converter, high-frequency-link power conversion, and flexible transmission and distribution system.

Mr. Zhao is a member of the IEEE Power Electronics Society, the Industrial Electronics Society, and the Chinese Society for Electrical Engineering.